Second-Order Spectral Statistics for the Power Gain of Wideband Wireless Channels

Milan S. Derpich and Rodolfo Feick

***Abstract*—We derive closed-form expressions for the second-order statistics of the power gain (as a function of frequency) of wide-band microwave indoor channels. We obtain our results within a framework general enough to be compatible with several popular channel models, such as the Saleh-Valenzuela channel model and those proposed by the IEEE 802.15.3a and IEEE 802.15.4a task groups. As in all these models, our channel description is based upon clusters and rays with (possibly mixed-) Poisson arrivals and random amplitudes. Our results consist of closed-form expressions for the second-order statistics of the channel power frequency response, where statistical averages involve expectations over ray amplitudes and arrival times. These expressions reveal that the auto-covariance of the spectral power gain between any two frequencies decreases and tends to zero as the difference between these frequencies tends to infinity if and only if the cluster arrival rate goes to infinity. They also show that the variance-to-squared-mean of the narrow-band power gain exhibits exactly the same behavior with respect to the center frequency. We then use these results to obtain closed-form expressions for the variance and second-order moment of the aggregate channel power gain over any given interval of frequencies. This allows us to express the channel spectral diversity as a function of model parameters and bandwidth. In addition, we illustrate how these equations allow one to devise automatic cluster identification algorithms which, from empirical estimates of the second-order spectral statistics of the channel power gain, can confirm or deny the existence of clusters in a given scenario.**

***Index Terms*—Statistical channel modeling, ultra-wideband channels, Sale-Valenzuela channel model, fading channels.**

I. Introduction

Stochastic wireless channel models allow one to predict the statistics of the radio propagation conditions over an ensemble of scenarios with similar characteristics. This is specially useful in complex, heterogeneous and time-varying environments, such as office, residential and industrial indoor scenarios.

One of the most popular models for indoor wireless channels is the one proposed by Saleh and Valenzuela in [1], which has served as the basis for several other channel models. Building upon it, the the IEEE 802.15.3a task group accepted a channel model [2] for ultra wide-band indoor communications, and similar models have been adopted for the IEEE 802.15.4a standard [3]. Like the Saleh-Valenzuela (SV) model, the IEEE 802.15.3a and the IEEE 802.15.4a channel models consist of a discrete-time description of the impulse response of a wireless channel, in which multi-path components are grouped into clusters[1].

Some of the useful time-domain delay-statistics of wireless channel models are the power delay profile, the average delay and the RMS delay, which, under suitable assumptions, allow one to determine spectral statistics such as coherence bandwidth and average power gain. These parameters, associated with second-order statistics of the channel impulse or frequency response, have been extensively discussed and characterized in the literature [4]–[7].

Another set of stochastic properties of wireless channels, which has received relatively less attention, are those derived from the second-order statistics of the channel *power* frequency response (that is, its squared frequency response magnitude, here denoted by $|H(j\omega)|^2$). An early analysis of these statistics and their application can be found in [8], where it is argued that the transmission over two carriers with the right frequency spacing may benefit from the negative correlation between each of the received powers. Simplified expressions for the spatial and spectral autocorrelation coefficients of $|H(j\omega)|^2$, as well as for its power over a frequency interval, are presented in [9], which are then evaluated via simulations. Building upon this result, and via simulations, it has been possible to assess fading depth statistics and relate them to bandwidth and to some features of the propagation environment [10], [11].

Although simulations of the second-order statistics of $|H(j\omega)|^2$ are helpful in assessing the performance of wireless communication systems, having *closed-form* expressions for these statistics provides further benefits. First (and naturally), such closed-form expressions can be substituted into other formulas, thus allowing one to relate them with performance indexes, also in closed form. Secondly, explicit parametric formulas will provide useful insight into the relationship between the performance of wireless communications systems and certain parameters. In particular, the second-order statistics of $|H(j\omega)|^2$ allow one to refine probabilistic approximations drawn from first-order statistics alone. Moreover if the power received over some band is known to distribute according to some parametric probability density function, then having the first- and second-order statistics of this power allows one to identify, in some cases, the parameters of the distribution [12]. This makes it possible to calculate fade-depth statistics from

Milan S. Derpich and Rodolfo Feick are with the Department of Electronic Engineering, Universidad Técnica Federico Santa María, Valparaíso, Chile. emails: {milan.derpich, rodolfo.feick}@usm.cl. The authors acknowledge the support of CONICYT project ACT-53, and FONDECYT project Nrs. 1095018 and 1120468.

[1]Except in the IEEE 802.15.4a channel model for frequencies below 1 GHz, see [3].

the second-order statistics of $|H(j\omega)|^2$. In this regard, it was already noted in [9]–[11], [13] that the fade depth decreases as the width of $\mathcal{B}$ is increased. In relation to this question, and using an information-theoretic approach and measured data, it has been shown in [14] that the number of significant eigenvalues of the covariance matrix of the random channel impulse response, and hence the diversity order of the channel, scales approximately linearly with bandwidth. Such an increase in diversity, which relates to the reduction of the relative channel power variance as the bandwidth increases, has been reported to reach a saturation point [12], [13], [15]. Having explicit expressions for this channel power variance as a function of bandwidth would allow one to predict the associated saturation bandwidth and relate it to environmental parameters.

Available closed-form results that allow one to analytically obtain the second-order statistics of $|H(j\omega)|^2$ are rather limited. Although the analysis in [9], [11] does obtain some intermediate closed-form expressions, the actual evaluation of these statistics is carried out by simulations. In addition, one of the simplifying assumptions underpinning the results in [9] and [11] is the uncorrelation between the amplitudes and arrival times of multi-path components, which is known to contradict channel measurements [1], [16]. Under the assumption of uncorrelated amplitudes and arrival times, and considering uniformly distributed arrival times, closed-form expressions for the autocorrelation of $|H(j\omega)|$ were derived in [17]. Exact closed-form expressions for all the joint moments between $|H(j\omega_1)|$ and $|H(j\omega_2)|$, for any frequencies ω_1, ω_2, as a function of the power delay profile of the channel impulse response have been found in [18], assuming that multipath-component amplitudes are independent jointly complex Gaussian and that arrival times are fixed. However, although popular channel models such as the SV model [1] consider complex Gaussian multipath component amplitudes, other amplitude distributions have been reported in the literature (see, e.g. [2]). Moreover, the conditional independence assumption in [18] does not hold for channel models where the impulse response exhibits clusters, such as the SV and its several extensions [1]–[3], [16]. In a recent paper [12], analytical expressions for the auto-correlation of the channel frequency response squared magnitude $|H(j\omega)|^2$, as well as the variance of the power over any frequency band, have been derived for the IEEE 802.15.4a channel model, conditioned to *fixed and given ray and cluster arrival times*. The corresponding statistics over random arrival times were obtained via simulations. To the best of the authors' knowledge, no closed-form expressions are available in the literature for second-order un-conditioned statistics of the spectral power gain of wireless channel models such as the IEEE 802.15.3a and IEEE 802.15.4a, as well as for other SV-like models.

In this paper, we derive closed-form exact expressions for the second-order statistics of $|H(j\omega)|^2$ for a general class of extensions of the SV channel model. This class includes, as special cases, those accepted by the IEEE 802.15.3a task group and the IEEE 802.15.4a channel modeling subgroup [2], [3], [16]. Unlike [12], our expressions include expectations considering the randomness of both ray amplitudes and arrival times. As in all SV-like models, our channel description is based upon clusters and rays, with different power decay profiles among and within clusters. Our analysis framework is general enough to encompass model features such as mixed-Poisson arrivals within clusters as well as models in which the first ray of each cluster exhibits statistics different from the other rays (these two features are considered in [3], [16], [19]). To this end, we first derive, in Section III, a general, exact and closed-form expression for the auto-covariance of $|H(j\omega)|^2$. This expression is determined by four functions, corresponding to the second- and fourth-order moment delay profiles of cluster and ray amplitudes multiplied by their respective arrival rates. We use these expressions to analyze the effect of having a finite/infinite number of clusters, as well as the implications of having only one cluster (or, equivalently, no clusters at all). We then use the former result to obtain, in Section IV, a closed-form expression for the variance and raw second-order moment of the channel power gain $P_{\mathcal{B}}$ integrated over any given interval of frequencies $\mathcal{B}$. Our derivations predict a positive lower bound for the ratio between the variance of $P_{\mathcal{B}}$ and its squared mean. This bound only vanishes as the arrival rate of clusters in the model tends to infinity, a result that is confirmed via simulations. (Some preliminary results on this topic were reported by the authors in [20]). In addition, the obtained equations allow one to devise an automatic cluster identification algorithm, capable of verifying or discarding the presence of clusters in an ensemble of channel impulse responses. Such an algorithm is illustrated in an example in Section V, and can be considered an alternative to other cluster identification algorithms, such as those proposed in [21], [22].

II. Channel Model

In this section we formulate the wireless channel-model framework to be be utilized throughout this work. The idea is to establish a framework general enough to encompass most of the SV-like models proposed in the available literature. With that idea in mind, and before proceeding, we will first review some of the salient features of several extensions of the SV model, from which we will then define the set of assumptions our results will be based upon.

A. Brief Review of SV-Like Channel Models

In all versions and extensions of the SV model, the channel is represented by a random impulse response of the form [1]–[3], [16]

$$\tilde{h}(\tau) = \sum\nolimits_{i=1}^{N_c} \sum\nolimits_{m=1}^{N_r} a_{i,m}\delta(\tau - \tau_{i,m}) \qquad (1)$$

where

$$\tau_{i,m} \triangleq T_i + t_{i,m}, \quad \forall i \in \{1,\ldots,N_c\}; \forall m \in \{1,\ldots,N_r\}$$

is the random arrival time of the m-th path (or ray) in the i-th cluster, $T_i \geq 0$ is the random arrival time of the i-th cluster, and $t_{i,m} \geq 0$ is the random delay of the m-th path in the i-th cluster relative to T_i. [2] Cluster and relative arrival times are

[2] For simplicity, we do not consider here a large-scale fading factor before the sum in (1). In [2], this shadowing term is a log-normal random variable independent of all the other random variables in the model, which can easily be incorporated to our results.

ordered, i.e., $T_i \geq T_j \iff i \geq j$ and $t_{i,m} \geq t_{i,n} \iff m \geq n$, $\forall i$. By definition, the cluster begins with its first ray, and thus

$$t_{i,1} = 0, \quad \forall i \in \{1, \ldots, N_c\}.$$

Each random coefficient $a_{i,m}$ in (1) represents the amplitude of the m-th path in cluster i. These random numbers are formed as

$$a_{i,m} = p_{i,m} A_i \alpha_{i,m}, \quad \forall i \in \{1, \ldots, N_c\}, \forall m \in \{1, \ldots, N_r\}. \tag{2}$$

Each $A_i \in \mathbb{R}_0^+$ is a random variable representing the amplitude of the i-th cluster, while each real-valued random variable $\alpha_{i,m} \geq 0$ denotes the amplitude (or gain) of the m-th multi-path component (or ray) within the i-th cluster relative to that cluster's amplitude. The meaning of the random numbers $\{p_{i,m}\}$ in (2) depends on whether a complex or a real base-band representation is used. For the former, $p_{i,m} = \mathrm{e}^{j\phi_{i,m}}$, where $\{\phi_{i,m}\}$ are i.i.d. uniformly distributed over $[-\pi, \pi]$ [1], [3], [16]. For the real base-band representation, which is regarded as more suitable for ultra-wideband applications, $\{p_{i,m}\}$ are binary random variables taking values from $\{-1, 1\}$ with equal probability [2]. In both cases,

$$\mathrm{E}\left[p_{i,m}\right] = 0, \quad \forall i, m. \tag{3}$$

B. Assumptions and Analysis Framework

In order to establish a framework to encompass the various features of the SV-like channel models present in [1]–[4], [16], [23] (and possible future ones), we will formulate now the least restrictive set of assumptions under which our analysis and results are valid. To do so, the following three definitions are necessary:

Definition 1 (Bounded-Density Markovian Process): We will say that a sequence of random arrival times $\{\mathrm{x}_k\}_{k=1}^{\infty}$, with $\mathrm{x}_i \geq \mathrm{x}_j \iff i \geq j$, is *bounded-density Markovian* if

i) The inter-arrival times $\{\mathrm{x}_{k+1} - \mathrm{x}_k\}_{k=1}^{\infty}$ satisfy the Markov chains

$$(\mathrm{x}_{k+1} - \mathrm{x}_k) \leftrightarrow \mathrm{x}_k \leftrightarrow \{\mathrm{x}_i\}_{i=1}^{k}, \quad k = 1, 2, \ldots$$

ii) There exists a constant $\rho < \infty$ such that, for every $\Delta > 0$ sufficiently small,

$$\frac{\Pr\{\mathrm{x}_{k+1} - \mathrm{x}_k < \Delta | \, \mathrm{x}_k = x\}}{\Delta} \leq \rho, \ \forall x \in \mathbb{R}_0^+, \ k = 1, \ldots$$

▲

In words, condition i) in the above definition requires that the inter-arrival time just after an arrival at x (and hence the arrival density at x) depends, at most, on the value of x. In turn, condition ii) guarantees that the arrival density at any $x \in \mathbb{R}_0^+$ is bounded.

Definition 2 (Sequence i.i.d. under another sequence): Let $\{\mathrm{x}_k\}_{k=1}^{\infty}$ be a bounded-density Markovian process, with x_1 possibly being deterministically equal to 0. We will say that a sequence of random variables $\{\varsigma_k\}_{k=1}^{\infty}$ is *i.i.d under* $\{\mathrm{x}_k\}_{k=1}^{\infty}$ if the next two conditions are satisfied:

i) The following Markov chains hold

$$\varsigma_k \leftrightarrow \mathrm{x}_k \leftrightarrow \varsigma_j, \quad \forall j \neq k, \ j, k = 1, 2, \ldots,$$

ii) For every $x \in \mathbb{R}_0^+$ and $m \in \mathbb{N}$, $\mathrm{E}\left[\varsigma_j^m | \, \mathrm{x}_j = x\right] = \mathrm{E}\left[\varsigma_k^m | \, \mathrm{x}_k = x\right]$, $\forall j, k \in \mathbb{S}$, where $\mathbb{S} \triangleq \{1, 2, \ldots\}$, if x_1 is random, and $\mathbb{S} \triangleq \{2, 3, \ldots\}$ if $\mathrm{x}_1 = 0$ deterministically.

▲

Notice that condition i) in Definition 2 corresponds to the conditional independence relationships between amplitudes and arrival times shared by all channel models considered in [1]–[4], [16], [23], [24], except the 802.15.4a model for industrial environments under LOS in [3], [16]. Similarly, taking $\{\varsigma_k\}_k$ as the cluster (or relative ray) amplitudes and the $\{\mathrm{x}_k\}_k$ as the cluster (or relative ray) arrival times, condition ii) encompasses all the amplitude distributions considered in [1]–[4], [16], [23], including the cases in which the amplitude of the first ray or cluster takes a special form, as in CM3 (body surface to body surface, 3.1-10.6 GHz) and CM4 (body surface to external, 3.1-10.6 GHz) in [24].

We will need one more definition in order to treat arrival-time distributions different from plain Poisson processes, such as mixed Poisson arrivals (described in (6) below). To this end, we introduce the following single and joint arrival density functions:

Definition 3 (Arrival Density Functions): Let $\{\mathrm{x}_k\}_{k=1}^{\infty}$ be a bounded-density Markovian sequence of arrival times, with x_1 possibly being equal to zero deterministically. For any $\Delta \geq 0$, denote the number of elements in $\{\mathrm{x}_k\}_{k=i}^{\infty}$ falling inside $[x, x + \Delta)$ by the random variable $\mathrm{n}_{\Delta}^{(i)}(x)$, $i \in \{1, 2\}$, i.e.,

$$\mathrm{n}_{\Delta}^{(i)}(x) \triangleq \left|\{\mathrm{x}_k\}_{k=i}^{\infty} \cap [x, x + \Delta)\right|,$$

where, for sets, $|\cdot|$ denotes cardinality. We define the single and joint *arrival density functions* of $\{\mathrm{x}_k\}_{k=1}^{\infty}$ as

$$\bar{\lambda}_{\mathrm{x}}(x) = \begin{cases} \bar{\lambda}_{\mathrm{x}}^{(1)}(x) & , \text{ if } \mathrm{x}_1 \text{ is random} \\ \bar{\lambda}_{\mathrm{x}}^{(2)}(x) + \delta(x) & , \text{ if } \mathrm{x}_1 = 0 \text{ deterministically} \end{cases} \tag{4a}$$

$$\bar{\bar{\lambda}}_{\mathrm{x}}(y, z) = \begin{cases} \bar{\bar{\lambda}}_{\mathrm{x}}^{(1)}(y, z) & , \text{if } \mathrm{x}_1 \text{ is random} \\ \bar{\bar{\lambda}}_{\mathrm{x}}^{(2)}(y, z) + \delta(y)\bar{\lambda}_{\mathrm{x}}^{(2)}(z) + \delta(z)\bar{\lambda}_{\mathrm{x}}^{(2)}(y), \text{ if} \\ \qquad\qquad \mathrm{x}_1 = 0 \text{ deterministically} \end{cases} \tag{4b}$$

where, for $i \in \{1, 2\}$,

$$\bar{\lambda}_{\mathrm{x}}^{(i)}(x) \triangleq \lim_{\Delta \to 0} \frac{\Pr\{\mathrm{n}_{\Delta}^{(i)}(x) \geq 1\}}{\Delta} \tag{5a}$$

$$\bar{\bar{\lambda}}_{\mathrm{x}}^{(i)}(y, z) \triangleq \begin{cases} \lim_{\Delta \to 0} \frac{\Pr\{\mathrm{n}_{\Delta}^{(i)}(y) \geq 1, \mathrm{n}_{\Delta}^{(i)}(z) \geq 1\}}{\Delta^2} & , \text{if } y \neq z \\ \lim_{\Delta \to 0} \frac{\Pr\{\mathrm{n}_{\Delta}^{(i)}(y) \geq 1, \mathrm{n}_{\Delta}^{(i)}(y+\Delta) \geq 1\}}{\Delta^2} & , \text{if } y = z \end{cases} \tag{5b}$$

▲

One case in which arrival times do not conform to a Poisson process is in the model proposed in [19] and further considered in [3], [16]. In that case, rays within each cluster are described

as having mixed Poisson arrivals, in which case the ray inter-arrival times are i.i.d. with probability density function

$$f_{\boldsymbol{t_{i,n+1}-t_n}}(t_{i,n+1}-t_{i,n}) = \begin{cases} \lambda_1 \, \mathrm{e}^{-\lambda_1(t_{i,n+1}-t_{i,n})} & \text{, with probability } \beta \\ \lambda_2 \, \mathrm{e}^{-\lambda_2(t_{i,n+1}-t_{i,n})} & \text{, with probability } 1-\beta \end{cases}, \quad \forall i, n = 1, 2, \ldots \tag{6}$$

where $\lambda_1, \lambda_2 \geq 0$ are two different Poisson arrival rates.

Making use of the above definitions we can now establish the scope of validity of our results by means of the following assumption:

Assumption 1: Cluster and ray arrival times and amplitudes are random and such that

i) The following independence relationships hold

$$p_{j,m} \perp\!\!\!\perp \{T_i, A_i, t_{i,n}, \alpha_{i,n}\}, \quad \forall i, j \in \{1, \ldots, N_c\}, \; \forall n, m \in \{1, \ldots, N_r\} \tag{7a}$$

$$p_{j,n} \perp\!\!\!\perp p_{i,m}, \quad \text{unless } j = i \text{ and } n = m, \tag{7b}$$

$$\alpha_{j,n} \perp\!\!\!\perp \alpha_{i,m}, \quad \text{unless } j = i, \tag{7c}$$

$$\{T_i, A_i\} \perp\!\!\!\perp \{t_{j,n}, \alpha_{j,n}\}, \quad \forall i, j \in \{1, \ldots, N_c\}, \; \forall n \in \{1, \ldots, N_r\} \tag{7d}$$

$$A_i \longleftrightarrow T_i \longleftrightarrow \{A_j, T_k, \alpha_{k,m}, t_{k,m}\}, \quad \forall i, j, k \in \{1, \ldots, N_c\}, m \in \{1, \ldots, N_r\} : \; i \neq j \tag{7e}$$

$$\alpha_{i,m} \longleftrightarrow t_{i,m} \longleftrightarrow \{A_k, T_k, \alpha_{j,n}, t_{k,m}\}, \quad \forall i, j, k \in \{1, \ldots, N_c\}, \; m, n \in \{1, \ldots, N_r\} : (i, m) \neq (j, n) \tag{7f}$$

where $\perp\!\!\!\perp$ denotes probabilistic independence, and where the Markov-chain notation $a \leftrightarrow b \leftrightarrow c$ means "a and c are independent when b is known".

ii) $\{T_i\}$ is a bounded-density Markovian sequence, with T_1 possibly deterministically equal to zero, with i.i.d inter-arrival times exponentially distributed with exponent Λ and with arrival density functions $\bar{\lambda}_T(\cdot)$, $\bar{\bar{\lambda}}_T(\cdot, \cdot)$.

iii) $\{t_{i,m}\}_{m=1}^{\infty}$ is a bounded-density Markovian sequence with $t_{i,1} = 0$ and arrival density functions $\bar{\lambda}_t(\cdot)$, $\bar{\bar{\lambda}}_t(\cdot, \cdot)$, for every $i \in \mathbb{N}$.

iv) $\{A_i\}_{i=1}^{\infty}$ is i.i.d. under $\{T_i\}_{i=1}^{\infty}$, with mth-order moment delay profile functions

$$b_m(x) \triangleq \begin{cases} \mathrm{E}\left[A_1^m\right], \\ \qquad \text{if } T_1 = 0 \text{ deterministically and } x = 0, \\ \mathrm{E}\left[A_k^m | T_k = x\right], k \in \{2, 3, \ldots\}, \\ \qquad \text{if } T_1 = 0 \text{ deterministically and } x \neq 0, \\ \mathrm{E}\left[A_k^m | T_k = x\right], k \in \{1, 2, \ldots\}, \\ \qquad \text{if } T_1 \text{ is random,} \end{cases} \tag{8a}$$

for $m \in \{1, 2\}$.

v) $\{\alpha_{i,n}\}_{n=1}^{\infty}$ is i.i.d. upon $\{t_{i,n}\}_{n=1}^{\infty}$, with mth-order moment delay profile functions

$$g_m(x) \triangleq \begin{cases} \mathrm{E}\left[\alpha_{i,1}^m\right], \quad \text{if } t_{i,1} = 0 \text{ deterministically and } x = 0, \\ \mathrm{E}\left[\alpha_{i,k}^m | t_{i,k} = x\right], k \in \{2, 3, \ldots\}, \\ \qquad \text{if } t_{i,1} = 0 \text{ deterministically and } x \neq 0, \\ \mathrm{E}\left[\alpha_{i,k}^m | t_{i,k} = x\right], k \in \{1, 2, \ldots\}, \text{ if } t_{i,1} \text{ is random,} \end{cases} \tag{8b}$$

where $m \in \{1, 2\}$, for every $i \in \mathbb{N}$. ▲

Notice that in the definitions within Assumption 1, the functions $b_m(\cdot)$ and $g_m(\cdot)$, $m = 1, 2$, capture the moment-delay profiles between clusters and within clusters, respectively, without taking arrival rates into account. In turn, the single and joint arrival rates of clusters are represented by the functions $\bar{\lambda}_T(\cdot)$ and $\bar{\bar{\lambda}}_T(\cdot, \cdot)$, while the single and joint relative arrival rates of rays are given by $\bar{\lambda}_t(\cdot)$ and $\bar{\bar{\lambda}}_t(\cdot, \cdot)$, respectively.

The requirements and suppositions in Assumption 1 are satisfied for all the channel models described in [1]–[4], [23], [24]. Indeed, by choosing cluster and ray arrival times as Poisson processes, with each $|\alpha_{i,m}|$ conditioned to $t_{i,m}$ being Rayleigh distributed with second moment $g_2(t) = \exp(-t/\gamma)$, and deterministic A_i's with the form $A_i = b_0 \exp(-T_i/\Gamma)$, $\Gamma, \gamma > 0$, we obtain the widely used Saleh-Valenzuela model [1]. A similar choice with log-normally distributed amplitudes $|A_i|$ and $|\alpha_i|$ yields the model proposed by the IEEE 802.15.3a task group [2] (excluding its large-scale fading term). The decay profiles of the amplitudes (represented by the functions b and g of (8)) can also be chosen to match those that the IEEE 802-15.4a standard recommends for high-frequencies in some scenario types (such as office and industrial) [16].

Remark 1: (Mixed Poisson Arrivals do ***not*** *Give Rise to a Mixed Poisson Distribution)* It is worth mentioning at this point that the mixed-Poisson arrivals, characterized by the conditional PDF given in (6), do **not** give rise to what is known as a mixed Poisson distribution [25]. More precisely, if the random exponent selection in (6) takes place after each arrival, then the probability of having n arrivals in any unit-length time interval $[x, x+1]$ cannot be written as $\beta p_n(\lambda_1) + (1-\beta) p_n(\lambda_2)$, where $p_n(\lambda)$ denotes the Poisson probability mass function with parameter λ. (The exact probability distribution has been derived by the first author in a work currently in preparation.) ▲

Another assumption that will facilitate the forthcoming analysis is related to the number of clusters and rays. Although in (1), as in [1], [2], [16], the number of clusters N_c and the number of paths within each cluster, N_r, are finite, we will consider infinitely many clusters and rays per cluster. As acknowledged in [1], the latter choice is arguably more realistic. Of course, this assumption requires that the amplitudes decay fast enough with increasing delay. We will make this requirement precise by assuming that the conditional moments

of the amplitudes defined in (8) satisfy

$$\int_0^\infty b_2(T)dT<\infty, \qquad \int_0^\infty b_4(T)dT<\infty$$
$$\int_0^\infty g_2(t)dt<\infty, \qquad \int_0^\infty g_4(t)dt<\infty,$$

and work in the sequel with the channel impulse response

$$h(t)\triangleq \sum\nolimits_{i=1}^{\infty}\sum\nolimits_{m=1}^{\infty} a_{i,m}\delta(t-\tau_{i,m}), \tag{9}$$

with $a_{i,m}$ and $\tau_{i,m}$ as defined in Section II-A. Also, as in [2], we will adopt a real baseband model for the impulse response, and hence the coefficients $p_{i,m}$ in (2) are i.i.d. Bernoulli random variables taking the values 1 or -1 with equal probability. This is done mainly to simplify notation, and it is worth mentioning that all forthcoming results also hold for the complex base-band representation (all that is required is that (3) and Assumption 1 hold).

From (9), the squared magnitude of the channel frequency response is

$$|H(j\omega)|^2=\sum_{i=1}^{\infty}\sum_{j=1}^{\infty}\sum_{m=1}^{\infty}\sum_{n=1}^{\infty} a_{i,m}a_{j,n}\,\mathrm{e}^{-j\omega(\tau_{i,m}-\tau_{j,n})} \tag{10}$$

A deterministic frequency-dependent gain for each ray, a feature discussed in [4], [16] and in [19], can be easily incorporated to our model by simply multiplying $|H(j\omega)|^2$ by the squared magnitude of this gain. For ease of notation, and because the effects of such factor on the resulting statistics can be easily added afterwards, we will not include it in our expressions.

In the following sections, and under Assumption 1, we will derive exact closed-form expressions for the second-order statistics of $|H(j\omega)|^2$ as well of the channel power over any given frequency interval, as a function of the moment delay functions b_2, b_4, g_2 and g_4.

III. Auto-Covariance of $|H(j\omega)|^2$

Here we will obtain closed-form expressions for the mean, auto-covariance, and auto-correlation coefficient of $|H(j\omega)|^2$ over any interval of angular frequencies. These results rely on several technical lemmas which can be found in the Appendix.

A. Expected value of $|H(j\omega)|^2$

From (10) and the zero-mean and independence properties of the polarities $\{p_i\}$ established in (7), it is easy to verify that

$$\mathrm{E}\left[|H(j\omega)|^2\right]=\sum\nolimits_{i=1}^{\infty}\sum\nolimits_{m=1}^{\infty}\mathrm{E}\left[a_{i,m}^2\right]. \tag{11}$$

Applying (2), the independence relationships (7d) and Lemma 1 (in the Appendix), it is readily found that

$$\begin{aligned}\mathrm{E}\left[|H(j\omega)|^2\right]&=\sum_{i=1}^{\infty}\mathrm{E}\left[A_i^2\right]\sum_{m=1}^{\infty}\mathrm{E}\left[\alpha_{i,m}^2\right]\\&=\left(\int_0^\infty \bar{\lambda}_T(x)b_2(x)dx\right)\left(\int_0^\infty \bar{\lambda}_t(x)g_2(x)dx\right).\end{aligned} \tag{12}$$

Thus, the expected value of $|H(j\omega)|^2$ is the same for all frequencies, being equal to the product of the average energy of the cluster amplitudes $\{A_i\}$ and the ray relative amplitudes $\{\alpha_{i,m}\}$.

B. Auto-covariance of $|H(j\omega)|^2$

Denote the auto-covariance of $|H(\omega)|^2$ by

$$\begin{aligned}c(\omega_1,\omega_2)\triangleq\ &\mathrm{E}\left[|H(\omega_1)|^2\,|H(\omega_2)|^2\right]\\&-\mathrm{E}\left[|H(\omega_1)|^2\right]\mathrm{E}\left[|H(\omega_2)|^2\right].\end{aligned} \tag{13}$$

The following theorem, which is the main result of this section, provides an exact, closed-form expression for $c(\omega_1,\omega_2)$ in terms of the arrival density functions $\bar{\lambda}_T$, $\bar{\bar{\lambda}}_T$ $\bar{\lambda}_t$, $\bar{\bar{\lambda}}_t$ and the moment-delay functions b_2, b_4, g_2 and g_4 defined in Assumption 1.

Theorem 1: Let clusters and rays distribute as in Assumption 1. Define the *effective moment delay profile functions*

$$\begin{aligned}B_m(x)&\triangleq \bar{\lambda}_T(x)b_m(x) \qquad \Psi(y,z)=\bar{\bar{\lambda}}_T(y,z)b_2(y)b_2(z)\\G_m(x)&\triangleq \bar{\lambda}_t(x)g_m(x) \qquad \Phi(y,z)\triangleq \bar{\bar{\lambda}}_t(y,z)g_2(y)g_2(z)\end{aligned} \tag{14}$$

for $m\in\{2,4\}$, and let $\widehat{B}_m$, $\widehat{G}_m$, $\widehat{\Psi}$ and $\widehat{\Phi}$, respectively, denote their Fourier transforms. Then, for any $\Omega,\Theta\in\mathbb{R}$,

$$\begin{aligned}c(\tfrac{\Theta+\Omega}{2},\tfrac{\Theta-\Omega}{2})&=\|B_4\|_1\left(\|G_4\|_1+\|\Phi\|_1\right)\\&\quad+\left(\|\Psi\|_1-\|B_2\|_1^2\right)\|G_2\|_1^2\\&\quad+\|B_4\|_1\widehat{\Phi}(\Omega,-\Omega)+\widehat{\Psi}(\Omega,-\Omega)\left|\widehat{G}_2(\Omega)\right|^2\\&\quad+\|B_4\|_1\widehat{\Phi}(\Theta,-\Theta)+\widehat{\Psi}(\Theta,-\Theta)\left|\widehat{G}_2(\Theta)\right|^2.\end{aligned} \tag{15}$$

Proof: See Section VII-A in the Appendix. ∎

Remark 2: Theorem 1 reveals that the variance of the channel power gain $|H(j\omega)|^2$ exhibits the same variation with ω as does its autocovariance $c(\frac{\Theta+\Omega}{2},\frac{\Theta-\Omega}{2})$ with Ω. Since the overall behavior of the latter is to decrease as Ω grows, it follows that the variability of the channel power gain is smaller at higher frequencies. Notice that this reduction does not come from the frequency-dependence affecting each multi-path component (which is typical of real indoor propagation channels [26]), since we have not included it in our model. However, had this dependence been included, the variance-to-squared-mean ratio of $|H(j\omega)|^2$ would still exhibit the decay with ω predicted by Theorem 1.[3] Instead, the origin of this behavior can be more intuitively understood by looking at (37) in the Appendix, and by recalling that $\mathrm{E}[|H(\omega)|^2]$ is independent of ω. In (37), if we choose $\omega_2=\omega_1=\omega$, then $\mathcal{T}_2(\omega_1+\omega_2)=\mathcal{T}_2(2\omega)$ becomes the only frequency-dependent term. Now, $\mathcal{T}_2(2\omega)$ is a sum of expectations of the random variables $a_\ell^2a_k^2\,\mathrm{e}^{-j2\omega[\tau_\ell-\tau_k]}$. At $\omega=0$, $\mathcal{T}_2$ turns into a sum of non-negative terms. By contrast, if we let ω increase so

[3] If this dependency can be captured by introducing a common impulse response for each multi-path component, say $f(t)$, with Fourier transform $F(j\omega)$, then the channel power gain becomes $|F(j\omega)|^2\,|H(j\omega)|^2$. With this, the mean channel power gain at ω is multiplied by $|F(j\omega)|^2$, and its autocovariance is to be computed as $|F(j\omega_1)|^2\,|F(j\omega_2)|^2\,c(\omega_1,\omega_2)$. Thus, in this case, the variance-to-squared-mean ratio would be unaffected by $F(j\omega)$ and would decay with ω as predicted by Theorem 1.

that the probability density functions of the random variables $2\omega[\tau_\ell - \tau_k]$ extend smoothly over an interval several times larger than 2π, then the phases of the exponentials will be approximately distributed uniformly over $[0, 2\pi]$. This will reduce each of the expectations in the sum. Thus, $\mathcal{T}_2(2\omega)$ decreases as ω grows, and so does $\mathrm{E}[|H(\omega_1)|^2 |H(\omega_2)|^2]$. ▲

Remark 3: If the effective moment delay functions G_m and B_m are "smooth", then all frequency-dependent terms in (15) vanish if $\omega_1 - \omega_2$ tends to infinity (while keeping $\omega_1, \omega_2 > 0$), leaving only $\|B_4\|_1 (\|G_4\|_1 + \|\Phi\|_1) + (\|\Psi\|_1 - \|B_2\|_1^2) \|G_2\|_1^2$. This implies that the auto-covariance between two infinitely distant frequency values is greater than zero, which, at first sight, may seem counter-intuitive. Nevertheless, and although this seems to be the first time such behavior is proven to exist for SV-like channel models, it is consistent with the saturation of the channel diversity order as the bandwidth increases, reported in [13], [15]. (Further treatment of this phenomenon is presented in Sections III-B3 and IV below.) As will be discussed in the following section, this non-zero asymptotic auto-covariance is due to the fact that the arrival rate of clusters is finite. ▲

We now apply these results to some specific cases.

1) Infinitely Many Clusters: Suppose the arrival densities of rays and clusters are scaled by $\nu > 0$ and $\mu > 0$, respectively, to obtain arrival rates

$$\bar{\lambda}_t'^{(1+q)}(x) \triangleq \nu \bar{\lambda}_t^{(1+q)}(x) \quad \bar{\bar{\lambda}}_t'^{(1+q)}(y,z) = \nu^2 \bar{\bar{\lambda}}_t^{(1+q)}(y,z)$$
$$\bar{\lambda}_T'^{(1+q)}(x) \triangleq \mu \bar{\lambda}_t^{(1+q)}(x) \quad \bar{\bar{\lambda}}_T'^{(1+q)}(y,z) = \nu^2 \bar{\bar{\lambda}}_T^{(1+q)}(y,z)$$

where

$$q \triangleq \begin{cases} 1 & , \text{ if } T_1 = 0 \text{ deterministically} \\ 0 & , \text{ otherwise.} \end{cases}$$

Let us also suppose that this is done while preserving the original power delay profiles (so that total impulse-response power is maintained), which requires one to scale g_2 and b_2 by ν^{-1} and μ^{-1}, respectively. This implies that the functions g_4 and b_4 are scaled by ν^{-2} and μ^{-2}, respectively. Denote the resulting scaled moment-profile densities by $B_2', B_4', G_2', G_4', \Phi', \Psi'$. Substituting into (14), the behavior of the terms involved in the frequency-independent part of (15) as cluster and ray densities go to infinity is given by the limits shown in (16) (next page). Therefore, for any given and smooth power-delay profile, $\lim_{|\omega_1-\omega_2|\to\infty} c(\omega_1, \omega_2) = 0$ if the cluster arrival rate tends to infinity and the *right-hand side* (RHS) of (16b) is zero. With this, as $\mu \to \infty$, in the case in which clusters have Poisson arrivals (which implies $\Psi(y,z) = B_2(y)B_2(z)$) and if the first cluster arrives randomly (i.e., if $q = 0$), then the autocovariance of $|H(j\omega)|^2$ takes the simpler form

$$c(\tfrac{\Theta+\Omega}{2}, \tfrac{\Theta-\Omega}{2}) = \left|\widehat{B_2}(\Omega)\right|^2 \left|\widehat{G}_2(\Omega)\right|^2 + \left|\widehat{B_2}(\Theta)\right|^2 \left|\widehat{G}_2(\Theta)\right|^2$$

That is, $c(\omega_1, \omega_2)$ reduces to the sum of the products of the squared magnitude Fourier transforms of the inter-cluster PDP and the intra-cluster PDP evaluated at $\omega_1 - \omega_2$ and at $\omega_1 + \omega_2$.

2) Only One Cluster / No Clusters: Consider the case in which rays do not exhibit the presence of clusters. This situation can be analyzed under the framework defined by Assumption 1 by supposing there is only one cluster with deterministic arrival time $T_1 = 0$ and amplitude $A_1 = 1$, and such that its first ray arrives deterministically at time $t_{1,1} = 0$. In order to ensure there are no other clusters, we may take $\mathrm{E}[A_k | T_k = T] = 0$, for all $k \in \{2, 3, \ldots\}$, for all $T \in \mathbb{R}_0^+$. With these choices, we obtain $B_2(x) = \delta(x)$, $B_4(x) = \delta(x)$, $\|B_4\|_1 = 1$, $\widehat{\Psi}(\theta, -\theta) = 0, \forall \theta \in \mathbb{R}$, and thus the auto-covariance becomes

$$c(\tfrac{\Theta+\Omega}{2}, \tfrac{\Theta-\Omega}{2}) = \|G_4\|_1 - \|G_2\|_1^2 + \|\Phi\|_1 + \widehat{\Phi}(\Omega, -\Omega) + \widehat{\Phi}(\Theta, -\Theta).$$

3) Non-Zero Asymptotic Autocovariance: As already mentioned in Remark 3, Theorem 1 reveals that, for finite cluster arrival rates, the autocovariance of $|H(j\omega)|$, that is, $c(\omega_1, \omega_2)$, tends to a positive value as $\omega_2 \to \infty$ (i.e., if Ω and Θ tend to ∞), and not to zero. To the best of our knowledge, this is the first time this result is derived or revealed, at least for SV-like channel models. (A simple and intuitive explanation of this phenomenon is provided at the beginning of Section IV-B below, in terms of the variance of the aggregate channel power gain over a given band). It is worth noting that such asymptotic behavior cannot be observed if one analyzes the autocovariance of the complex frequency response $H(j\omega)$, i.e., by looking at the second-order statistics of $H(j\omega)$ instead of those of $|H(j\omega)|^2$. Indeed, applying the independence relationships (7a) and (7d), and then Lemma 1, it becomes easy to show that

$$\mathrm{E}[H(j\omega_1)H^*(j\omega_2)] = \widehat{B}_2(\omega_1 - \omega_2)\widehat{G}_2(\omega_1 - \omega_2).$$

This simple expression (which we believe to be novel), implies that, if the moment-delay profiles of clusters and rays within them are smooth, then $\lim_{|\omega_1-\omega_2|\to\infty} \mathrm{E}[H(j\omega_1)H^*(j\omega_2)] = 0$.

C. Correlation Coefficient of $|H(j\omega)|^2$

The correlation coefficient of $|H(j\omega)|^2$, denoted by $\rho(\omega_1, \omega_2)$, is given by

$$\rho(\omega_1, \omega_2) \triangleq \frac{c(\omega_1, \omega_2)}{\sqrt{var(|H(j\omega_1)|^2) var(|H(j\omega_2)|^2)}} \quad (17)$$

From (13), it readily follows that (17) can be written as

$$\rho(\omega_1, \omega_2) = \frac{c(\omega_1, \omega_2)}{\sqrt{c(\omega_1, \omega_1)c(\omega_2, \omega_2)}}, \quad \forall \omega_1, \omega_2 \geq \omega_{min} \quad (18)$$

It was already shown that for any given smooth moment-delay profile functions, the auto-covariance between two frequencies ω_1 and $\omega_1 + \Omega$ tends to zero as $\Omega \to \infty$ if the cluster arrival density goes to infinity. We shall see in Section V-A that even when this arrival density is finite, $\lim_{\Omega\to\infty} \rho(\omega_1, \omega_2 + \Omega) = 0$ if the moment delay profiles change so that the number of clusters with significant amplitude tends to infinity.

$$\lim_{\mu\to\infty}\|B_4'\|_1 = \lim_{\mu\to\infty}\int\left(\mu\bar{\lambda}_T^{(1+q)}(y)+q\delta(y)\right)\mu^{-2}b_4(y)dy = 0 \tag{16a}$$

$$\begin{aligned}\lim_{\mu\to\infty}(\|\Psi'\|_1-\|B_2'\|_1^2) &= \lim_{\mu\to\infty}\iint\left(\mu^2\bar{\bar{\lambda}}_T^{(1+q)}(y,z)-\mu^2\bar{\lambda}_T(y)\bar{\lambda}_T(z)-q\,\delta(y)\delta(z)\right)\mu^{-2}b_2(y)b_2(z)dydz\\ &= \|\Psi\|_1-\|B_2\|_1^2+q\,b_2(0)^2\end{aligned} \tag{16b}$$

$$\lim_{\nu\to\infty}\|G_4'\|_1 = \lim_{\nu\to\infty}\int(\nu\bar{\lambda}_t^{(1+q)}(y)+q\delta(y))\nu^{-2}g_4(y)dy = 0 \tag{16c}$$

$$\begin{aligned}\lim_{\nu\to\infty}\|\Phi'\|_1 &= \lim_{\nu\to\infty}\iint(\nu^2\bar{\bar{\lambda}}_t^{(1+q)}(y,z)+q\nu\delta(y)\bar{\lambda}_t^{(1+q)}(z)+q\nu\delta(z)\bar{\lambda}_t^{(1+q)}(y))\nu^{-2}g_2(y)g_2(z)dydz\\ &= \iint\bar{\bar{\lambda}}_t^{(1+q)}(y,z)g_2(y)g_2(z)dydz>0\end{aligned} \tag{16d}$$

IV. Second-Order Statistics Over a Frequency Band

In this section we will use Theorem 1 to derive closed-form expressions for the mean and variance of the total channel power over any given frequency band

$$\mathcal{B}\triangleq[\omega_l,\omega_r]\subset[0,\infty),\quad 0\le\omega_l\le\omega_r,$$

where ω_l and ω_r are in [rad/s].

A. Expected Value of the Channel Power Over a Frequency Band

Denote the channel power over the frequency band $\mathcal{B}$ by $P_{\mathcal{B}}\triangleq\int_{\omega_l}^{\omega_r}|H(j\omega)|^2\,d\omega$. Given the fact that $\mathrm{E}\left[|H(j\omega)|^2\right]$ is constant for all $\omega\in\mathbb{R}$ (see (11)), it follows from (12) that

$$\begin{aligned}\mathrm{E}[P_{\mathcal{B}}] &= W\left(\int_0^\infty\bar{\lambda}_T(x)b_2(x)dx\right)\left(\int_0^\infty\bar{\lambda}_t(x)g_2(x)dx\right)\\ &= W\|B_2\|_1\|G_2\|_1,\end{aligned}$$

where

$$W\triangleq|\mathcal{B}|=\omega_r-\omega_l.$$

B. Variance of the Channel Power Over a Frequency Band

The variance of the channel power over a band $\mathcal{B}\triangleq[\omega_l,\omega_r]$ can be obtained directly from the auto-covariance of $|H(j\omega)|^2$ as

$$var(P_{\mathcal{B}})=\int_{\mathcal{B}}\int_{\mathcal{B}}c(\omega,u)d\omega du. \tag{19}$$

Before proceeding, it is worth noting that (19) readily implies that, if $c(\omega,u)$ is bounded, then

$$\lim_{|\omega-u|\to\infty}c(\omega,u)=0\Longrightarrow\lim_{|\mathcal{B}|\to\infty}\frac{var(P_{\mathcal{B}})}{\mathrm{E}[P_{\mathcal{B}}]^2}=0, \tag{20}$$

since $\mathrm{E}[P_{\mathcal{B}}]$ grows linearly with $|\mathcal{B}|$. This allows one to provide a simple and intuitive explanation for the fact that $c(\omega,u)$ (i.e., the autocovariance of $|H(j\omega)|^2$) does not vanish when the two frequencies $\omega,u\ge 0$ are infinitely distant from one another. Recall from Parseval's theorem that when $|\mathcal{B}|\to\infty$, $P_{\mathcal{B}}$ equals the total impulse-response power. Then, if the impulse response is amplitude-modulated by a finite number of random-amplitude cluster envelopes, it is clear that the ratio variance of impulse-response power over the square of the expected impulse-response power will not be zero. In view of (20), this will imply that $\limsup_{|\omega-u|\to\infty}c(\omega,u)\neq 0$. That is, the autocovariance of $|H(j\omega)|^2$ between a pair of infinitely-distant frequencies will not be zero whenever the total number of clusters with random amplitude remains finite. As anticipated, this provides an alternative and more intuitive explanation to what was already discussed in Section III-B3.

We now return to characterizing the variance of $P_{\mathcal{B}}$. From (15), $c(\omega_1,\omega_2)$ can be written as

$$c(\tfrac{\Theta+\Omega}{2},\tfrac{\Theta-\Omega}{2})=K+\bar{c}(\Omega)+\bar{c}(\Theta) \tag{21}$$

where

$$K\triangleq=\|B_4\|_1\left(\|G_4\|_1+\|\Phi\|_1\right)+\left(\|\Psi\|_1-\|B_2\|_1^2\right)\|G_2\|_1^2 \tag{22a}$$

$$\bar{c}(\omega)\triangleq\|B_4\|_1\widehat{\Phi}(\omega,-\omega)+\widehat{\Psi}(\omega,-\omega)\left|\widehat{G_2}(\omega)\right|^2 \tag{22b}$$

Substitution of (21) into (19) yields

$$var(P_{\mathcal{B}})=W^2K+\int_{\mathcal{B}}\int_{\mathcal{B}}\bar{c}(\omega-u)d\omega du+\int_{\mathcal{B}}\int_{\mathcal{B}}\bar{c}(\omega+u)d\omega du.$$

Recalling the change of variables $\Omega=\omega-u$, $\Theta=\omega+u$, and integrating along diagonal strips over the square $[\omega_l,\omega_r]\times[\omega_l,\omega_r]$, we obtain

$$\begin{aligned}var(P_{\mathcal{B}}) &= W^2K+2\int_0^W(W-u)\bar{c}(u)du\\ &\quad+\int_{\omega_l}^{\omega_r}\bar{c}(\omega_l+u)(u-\omega_l)du+\int_{\omega_l}^{\omega_r}\bar{c}(u+\omega_r)(\omega_r-u)du\end{aligned} \tag{23}$$

We note that $var(P_{\mathcal{B}})$ is a measure of the fluctuation of the received power over a wireless channel, and that the latter defines its fade statistics. The fact that fade depth decreases with channel bandwidth has been reported in the literature, both from empirical data (see, e.g., [13]) as well as using simulations [12], [27]. However, a closed-form formula relating fade depth and the classical channel model parameters used here has, to the best of our knowledge, not been reported

to date. The results derived above allow us to directly deal with this issue, provided the fading distribution can be fully determined from its second moment (an assumption which was successfully applied in [12]). The explicit dependency between $var(P_{\mathcal{B}})$ and W is illustrated in the example in the following section.

V. Example

In this section we will illustrate the application of the results obtained in sections III and IV to the "classical" Saleh-Valenzuela model [1]. In particular, we will show that our analytical expressions found in sections III and IV accurately predict the autocovariance of $|H(j\omega)|^2$ and the variance of the channel power gain over any given band. Also, we will show how the presence of clusters can be confirmed or discarded by using the second-order statistics of $|H(j\omega)|^2$ and the expressions derived in this work.

A. Model Parameters

In the SV model, the amplitudes $|\alpha_{i,m}|$ are Rayleigh distributed (conditioned to $t_{i,m}$), and the A_i's are deterministic exponentially decaying. The power delay profiles of cluster and ray amplitudes are given by

$$b_2(T) = A_i^2|_{T_i=T} = \mathrm{e}^{-T/\Gamma}$$
$$g_2(t) = \mathrm{E}\left[\alpha_{i,m}^2 | t_i = t\right] = \mathrm{e}^{-t/\gamma}$$

For the fourth-order moments we have

$$b_4(T) = \mathrm{E}\left[A_i^4 | T_i = T\right] = \mathrm{e}^{-2T/\Gamma}$$
$$g_4(T) = \mathrm{E}\left[\alpha_{i,m}^4 | t_{i,m} = t\right] = 2\,\mathrm{e}^{-2t/\gamma}$$

where the last equation follows since the fourth moment $\mathrm{E}\left[x^4\right]$ of a Rayleigh distributed random variable x is related to its second-order moment as $\mathrm{E}\left[x^4\right] = 2\,\mathrm{E}\left[x^2\right]^2$. Both cluster and relative ray inter arrival times are i.i.d. exponentially distributed with exponents Λ and λ, respectively. Also, the arrival times of the first cluster and the relative arrival time of the first ray in every cluster are, by definition, zero. Therefore, the effective moment profile functions defined in (14) take the form

$$B_2(T) = (\Lambda + \delta(T))b_2(T) = \Lambda\,\mathrm{e}^{-T/\Gamma} + \delta(T) \tag{24a}$$
$$B_4(T) = (\Lambda + \delta(T))b_4(T) = \Lambda\,\mathrm{e}^{-2T/\Gamma} + \delta(T) \tag{24b}$$
$$\begin{aligned}\Psi(y,z) &= (\Lambda^2 + \Lambda\delta(y) + \Lambda\delta(z))b_2(y)b_2(z)\\ &= B_2(y)B_2(z) - \delta(y)\delta(z)\end{aligned} \tag{24c}$$
$$G_2(t) = (\lambda + \delta(t))g_2(t) = \lambda\,\mathrm{e}^{-t/\gamma} + \delta(t) \tag{24d}$$
$$G_4(t) = (\lambda + \delta(t))g_4(t) = 2\lambda\,\mathrm{e}^{-2t/\gamma} + 2\delta(t) \tag{24e}$$
$$\begin{aligned}\Phi(y,z) &= (\lambda^2 + \lambda\delta(y) + \lambda\delta(z))g_2(y)g_2(z)\\ &= G_2(y)G_2(z) - \delta(y)\delta(z)\end{aligned} \tag{24f}$$

B. Auto-covariance

Recall from (21) that $c(\omega_1, \omega_2)$ can be written as

$$c(\tfrac{\Theta+\Omega}{2}, \tfrac{\Theta-\Omega}{2}) = K + \bar{c}(\Omega) + \bar{c}(\Theta) \tag{25}$$

In this case, from (22),

$$\begin{aligned}K &= \|B_4\|_1\left(\|G_4\|_1 + \|\Phi\|_1\right) + \left(\|\Psi\|_1 - \|B_2\|_1^2\right)\|G_2\|_1^2\\ &= \|B_4\|_1\left(\|G_4\|_1 + \|G_2\|_1^2 - 1\right) - \|G_2\|_1^2\\ &= (\tfrac{\Lambda\Gamma}{2} + 1)\left(\lambda\gamma + 2 + (\lambda\gamma+1)^2 - 1\right) - (\lambda\gamma+1)^2\\ &= \tfrac{\Lambda\Gamma}{2}(\lambda\gamma+1)^2 + (\tfrac{\Lambda\Gamma}{2}+1)(\lambda\gamma+1)\end{aligned} \tag{26}$$

$$\begin{aligned}\bar{c}(\omega) &= \|B_4\|_1\widehat{\Phi}(\omega,-\omega) + \widehat{\Psi}(\omega,-\omega)\left|\widehat{G}_2(\omega)\right|^2\\ &= \|B_4\|_1\left(\left|\widehat{G}_2(\omega)\right|^2 - 1\right) + \left(\left|\widehat{B}_2(\omega)\right|^2 - 1\right)\left|\widehat{G}_2(\omega)\right|^2\\ &= (\tfrac{\Lambda\Gamma}{2}+1)\left(\frac{\lambda^2 + 2\lambda/\gamma}{1/\gamma^2+\omega^2}\right)\\ &\qquad + \left(\frac{\Lambda^2 + 2\Lambda/\Gamma}{1/\Gamma^2+\omega^2}\right)\left(\frac{\lambda^2+2\lambda/\gamma}{1/\gamma^2+\omega^2} + 1\right)\\ &= (\tfrac{\Lambda\Gamma}{2}+1)\left(\frac{\lambda^2 + 2\lambda/\gamma}{1/\gamma^2+\omega^2}\right)\\ &\quad + \left(\frac{\Lambda^2 + 2\Lambda/\Gamma}{1/\Gamma^2+\omega^2}\right)\left(\frac{\lambda^2+2\lambda/\gamma}{1/\gamma^2+\omega^2}\right) + \left(\frac{\Lambda^2 + 2\Lambda/\Gamma}{1/\Gamma^2+\omega^2}\right)\end{aligned}$$

If $\gamma \neq \Gamma$, the decomposition into partial fractions of the term

$$\begin{aligned}&\frac{1}{(1/\Gamma^2+\omega^2)(1/\gamma^2+\omega^2)}\\ &\qquad = \frac{1}{1/\gamma^2 - 1/\Gamma^2}\left(\frac{1}{1/\Gamma^2+\omega^2} - \frac{1}{1/\gamma^2+\omega^2}\right)\end{aligned}$$

allows one to write

$$\begin{aligned}\bar{c}(\omega) &= (\tfrac{\Lambda\Gamma}{2}+1)\left(\frac{\lambda^2+2\lambda/\gamma}{1/\gamma^2+\omega^2}\right)\\ &\quad + \frac{(\Lambda^2+2\Lambda/\Gamma)(\lambda^2+2\lambda/\gamma)}{1/\gamma^2-1/\Gamma^2}\times\left(\frac{1}{1/\Gamma^2+\omega^2} - \frac{1}{1/\gamma^2+\omega^2}\right)\\ &\qquad + \left(\frac{\Lambda^2+2\Lambda/\Gamma}{1/\Gamma^2+\omega^2}\right)\\ &= (\tfrac{\Lambda\Gamma}{2}+1)\left[\frac{\lambda^2+2\lambda/\gamma}{1/\gamma^2+\omega^2} + \frac{2\Lambda/\Gamma(\lambda^2+2\lambda/\gamma)}{1/\gamma^2-1/\Gamma^2}\times\right.\\ &\qquad \left.\left(\frac{1}{1/\Gamma^2+\omega^2} - \frac{1}{1/\gamma^2+\omega^2}\right) + \frac{2\Lambda/\Gamma}{1/\Gamma^2+\omega^2}\right]\\ &= \underbrace{(\tfrac{\Lambda\Gamma}{2}+1)(\lambda^2+2\lambda/\gamma)\left[1 - \frac{2\Lambda\Gamma}{\frac{\Gamma^2}{\gamma^2}-1}\right]}_{K_1}\frac{1}{1/\gamma^2+\omega^2}\\ &\quad + \underbrace{(\tfrac{\Lambda\Gamma}{2}+1)2\Lambda\Gamma\left[\frac{\lambda^2+2\lambda/\gamma}{\frac{\Gamma^2}{\gamma^2}-1} + \frac{1}{\Gamma^2}\right]}_{K_2}\frac{1}{1/\Gamma^2+\omega^2}\end{aligned} \tag{27}$$

Substitution of this result into (25) yields

$$\begin{aligned}c(\tfrac{\Theta+\Omega}{2}, \tfrac{\Theta-\Omega}{2}) &= K + \frac{K_1}{1/\gamma^2+\Omega^2} + \frac{K_2}{1/\Gamma^2+\Omega^2}\\ &\quad + \frac{K_1}{1/\gamma^2+\Theta^2} + \frac{K_2}{1/\Gamma^2+\Theta^2}\end{aligned} \tag{28}$$

Figure 1 shows (with dashed-line curves) the empirical estimates of $c(\cdot,\cdot)$ of the SV channel model with four different

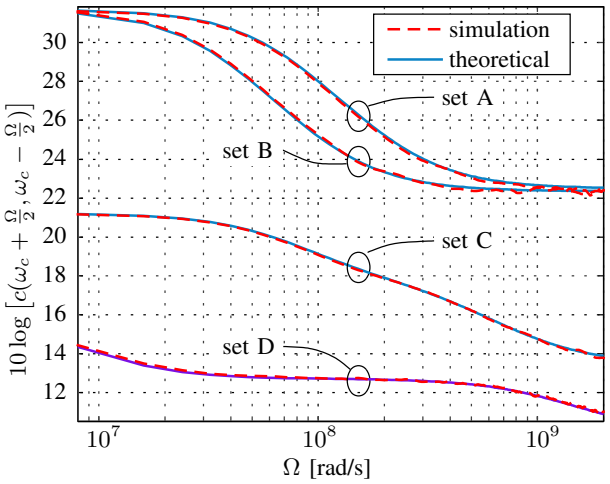

Figure 1: Spectral autocovariance of $|H(j\omega)|^2$ as a function of the frequency separation Ω (around a central frequency $\omega_c = 10^9$ [rad/s]) for the SV model with the four sets of parameters shown in Table I. Simulated curves (in dashed line) are averages over 300.000 channel realizations. Each theoretical curve (in solid line) was obtained using (28).

Set	Λ (ns^{-1})	Γ (ns)	λ (ns^{-1})	γ (ns)
A	0.06670	14	2.10	7.9
B	0.03335	28	1.05	15.8
C	0.06670	14	2.10	1.975
D	0.00667	140	2.10	0.79

Table I: Sets of parameters for the SV model used for the simulations in this section.

sets of parameters, specified in Table I. Each of these curves was obtained after 300000 simulated random realizations of channel impulse response. On the same plot, the theoretical values of $c(\cdot,\cdot)$ predicted by (28) are traced using solid lines, for each set of parameters. It can be seen that, in all cases, (28) matches the simulated data very tightly.

The set A of parameters corresponds to those proposed in the IEEE802.15.3a CM3 [2]. Notice that for the curves of this set, as Ω is increased, the spectral autocovariance drops by approximately 3 [dB] when $\Omega = 1/\Gamma = 7.14\times10^7$ [rad/s], and then decays at about 10 [dB] per decade, which is precisely the behavior determined by (28) (provided K_2 is much larger than K_1 and K). From (28), the next corner separation frequency, beyond which $c(\cdot,\cdot)$ almost ceases to diminish, takes place when $(K_1+K_2)/\Omega^2 \simeq K$, which in this case corresponds to $\Omega \simeq 2.1\times10^8$ rad/s], in agreement with what is shown in Fig. 1. The set B of curves differs from the previous one in that the arrival rates are halved, while the decay exponents are doubled. This yields, the same products $\Lambda\Gamma$ and $\lambda\gamma$ and the same ratio Γ/γ as the set A. Thus, the constants K, $K_1\gamma^2$ and $K_2\Gamma^2$ are also the same as those yielded by the set A parameters. Accordingly, the only difference with respect with the set-A curves is that the corner frequencies are reduced by a factor of two. Also as predicted by (28), reducing γ to one fourth of its value in set A increased the corner frequency $1/\gamma$ associated with K_1 by four, sufficiently higher than $1/\Gamma$ to have a small but noticeable effect (see the slight "bump" in the set-C curves between 2×10^8 and 7×10^8 [rad/s]. With the parameters of set D, these two corner frequencies are two-decades away from one another, with their presence becoming clearly visible in the corresponding plot in Fig. 1. Intuitively, the existence of two corner separation frequencies beyond which the spectral autocovariance starts (or restarts) to decrease can be associated with the temporal resolution associated with Ω. More precisely, when Ω is too small, all rays in the impulse response are added with roughly the same phase in the sum (10) for $\omega_c+\Omega/2$ and for $\omega_c-\Omega/2$, yielding a high correlation. As Ω is increased, a point is reached ($\Omega \simeq 1/\Gamma$) at which some clusters within the impulse response contribute with different random phases in (10), which begins to decorrelate the channel power gains. This reduction ceases when Ω is large enough so that all clusters within the impulse response are added with different phases, restarting only when Ω begins to make also the rays *within* each cluster add with different random phases ($\Omega \simeq 1/\gamma$).

C. Correlation Coefficient

The variance of $|H(j\omega)|^2$ is directly obtained by evaluating (28) for an arbitrary frequency $\omega/2$, which yields

$$var(|H(j\omega/2)|^2) = c(\tfrac{\omega}{2},\tfrac{\omega}{2}) = K + K_1\gamma^2 + K_2\Gamma^2 + \frac{K_1}{1/\gamma^2+\omega^2} + \frac{K_2}{1/\Gamma^2+\omega^2}$$

Substituting this and (28) into (18), the correlation coefficient takes the form shown in (29), displayed on the next page. Substituting the definitions of K, K_1 and K_2 into this expression, and after some algebra, one obtains that the correlation coefficient satisfies

$$\lim_{\omega\to\infty}\rho(\omega_1,\omega_1+\omega) = \frac{K}{K+K_1\gamma^2+K_2\Gamma^2} = \frac{\frac{\Lambda\Gamma}{2}(\lambda\gamma+1)^2+(\frac{\Lambda\Gamma}{2}+1)(\lambda\gamma+1)}{(\lambda\gamma+1)^2\{(\Lambda\Gamma+1)^2+\Lambda\Gamma\}+(\frac{\Lambda\Gamma}{2}+1)\lambda\gamma}$$

Thus, extending what was found for the autocovariance of $|H(j\omega)|^2$ in Section III-B1, we see here that the lower asymptote of the spectral power correlation as $\Omega\to\infty$ vanishes not only when $\Lambda\to\infty$, but also when the product $\Lambda\Gamma\to\infty$. Moreover, for any $\omega_1\in\mathbb{R}$, we have that $\lim_{\Omega\to\infty}\rho(\omega_1,\omega_1+\Omega)=0$ if and only if $\Lambda\Gamma\to\infty$.

D. Clusters or no Clusters?

When analyzing a sufficiently large number of realizations of the impulse response of a wireless channel, the only SV-model parameters which can be directly estimated are the ray arrival rate λ and the inter-cluster decay exponent Γ. In contrast, the inter-cluster arrival rate Λ, the intra-cluster decay exponent γ are not readily observable. Indeed, the very existence of clusters is not unquestionably evident from the impulse response realizations.

In this section, and based upon the results above, we propose a quantitative method for estimating γ, Λ. By doing this, it is possible to assert the presence of clusters (if the value $1/\Lambda$

$$\rho(\tfrac{\Theta-\Omega}{2},\tfrac{\Theta+\Omega}{2}) = \frac{K+\frac{K_1}{1/\gamma^2+\Omega^2}+\frac{K_2}{1/\Gamma^2+\Omega^2}+\frac{K_1}{1/\gamma^2+\Theta^2}+\frac{K_2}{1/\Gamma^2+\Theta^2}}{\sqrt{\left[K+K_1\gamma^2+K_2\Gamma^2+\frac{K_1}{1/\gamma^2+(\Theta-\Omega)^2}+\frac{K_2}{1/\Gamma^2+(\Theta-\Omega)^2}\right]\left[K+K_1\gamma^2+K_2\Gamma^2+\frac{K_1}{1/\gamma^2+(\Theta+\Omega)^2}+\frac{K_2}{1/\Gamma^2+(\Theta+\Omega)^2}\right]}}. \quad (29)$$

obtained is comparable to or smaller than Γ) or the absence of them (if $1/\Lambda \gg \Gamma$).[4]

As already said, the inter-cluster decay profile Γ and the intra-cluster arrival rate λ can be estimated directly from measurements (as done in, e.g., [1], [19]). Additional equations for finding the remaining two parameters (Λ and γ), can be generated by evaluating $c(\Omega,\Omega)$ at two or more different frequencies.[5] For the SV channel model considered in this example, the two simplest equations can be obtained from (28), as

$$L_1(\Lambda\Gamma,\lambda\gamma) \triangleq \mathrm{E}\left[|H(j\omega)|^2\right] = (\Lambda\Gamma+1)(\lambda\gamma+1) \quad (30)$$

$$L_2(\Lambda\Gamma,\lambda\gamma) \triangleq \lim_{\Theta,\Omega\to\infty} c(\tfrac{\Theta+\Omega}{2},\tfrac{\Theta-\Omega}{2}) = K = \tfrac{\Lambda\Gamma}{2}(\lambda\gamma+1)^2 + \left(\tfrac{\Lambda\Gamma}{2}+1\right)(\lambda\gamma+1) \quad (31)$$

The left-hand sides of these expressions (L_1 and L_2) can be directly estimated from measurements. Denote these estimates as $\hat{L}_1$ and $\hat{L}_2$, respectively. In principle, one could express $\Lambda\Gamma$ and $\lambda\gamma$ in closed form as functions of L_1 and L_2, and then evaluate for $L_1=\hat{L}_1$, $L_2=\hat{L}_2$. However, $\lambda\gamma$ is in this case the solution to the quadratic equation

$$(\lambda\gamma+1)^2-(L_1+1)(\lambda\gamma+1)+2L_2-L_1=0, \quad (32)$$

resulting from substituting (30) into (31). Therefore, the approximate nature of $\hat{L}_1,\hat{L}_2$ can turn a real positive root of (32) into a complex-valued (or negative) one. Moreover, even if one could measure L_1 and L_2 with infinite precision, there can still be two real-valued roots of (32) greater than 1. To overcome these difficulties, the following algorithm is proposed:

i) Find each of the p local minimizers of

$$\left|(\lambda\gamma)^3+(2-\hat{L}_1)(\lambda\gamma)^2+(2\hat{L}_2-3\hat{L}_1+2)\lambda\gamma+2\hat{L}_2-\hat{L}_1+1\right|$$

(the magnitude of the LHS of (32) with the estimates for L_1 and L_2). Denote these minimizers as $\tilde{y}_1,\ldots,\tilde{y}_p$, respectively, where $p\in\{1,2\}$. From these, calculate the non-negative pseudo-minimizers $y_i \triangleq \max\{0\,,\,\tilde{y}_i\}, i=1,\ldots,p$. These will be the preliminary candidates for $\lambda\gamma$.

ii) Let $x_i=\hat{L}_1/(y_i+1)-1$, $i=1,\ldots,p$, be the corresponding preliminary candidates for $\Lambda\Gamma$.

iii) For each $i=1,\ldots,p$: let $\Lambda_i=x_i/\Gamma$ and $\gamma_i=y_i/\lambda$. Then apply a least-squares curve-fitting optimization algorithm, with Λ and γ as unknowns, to match (28) against the empirical estimates of $c(\cdot,\cdot)$ at several frequencies. Use Λ_i and γ_i as initial values. Define the obtained residual matching errors as ϵ_i

iv) Pick the values of Λ_i,γ_i associated with the minimum ϵ_i.

This technique for estimating $\Lambda\Gamma$ and $\lambda\gamma$ was applied to simulated impulse responses for the SV channel model, with two sets of parameters. For the first of these (set E), $\Lambda=1.1$ ns^{-1}, $\lambda=1.1$ ns^{-1}, $\Gamma=14$ ns, and $\gamma=7.9$ ns. Notice that this makes $\Lambda=\lambda$, i.e., the clusters arrive at the same rate as the multi-path components within them, making it very difficult to distinguish one cluster from another in the time domain.

It may be noticed that the chosen inter-cluster and intra-cluster decay exponents (Γ and γ) are the same as those from the the IEEE802.15.3a CM3 [2] used in Section V-B. In turn, the product $\lambda\Lambda$ has been chosen about ten times larger than that used in Section V-B, so that the resulting dense train of rays makes it even harder to recognize the presence of clusters. A typical channel impulse response obtained for these parameters is shown in Fig. 2-top-left. As anticipated, with the chosen parameters, clusters arrive so densely that it is virtually impossible to tell one from the other. After simulating twelve sets of 4000 independent realizations of these impulse responses, estimates of L_1 and L_2 were obtained by averaging. From the corresponding twelve empirical estimates of $c(0,\omega)$, obtained for 500 values of ω evenly distributed from 0 to 5×10^9 rad/s, the parameters $\Lambda\Gamma$ and $\lambda\gamma$ were estimated using the method described above, yielding the results shown in the scatter plot of Fig. 2-top-right. The average error magnitude of these estimates is less than 30% of their true values.[6] More importantly, in all cases, the existence of clusters is unambiguously revealed, since all estimates of $\Lambda\Gamma$ are greater than 13. This seems more remarkable after recalling that, in this case, the impulse responses are such that clusters are almost totally overlapped, making it virtually impossible to distinguish one from the other.

The results for a scenario in which there are no clusters is shown in Fig. 2-bottom. I this case, the set F of parameters is used for the SV model: $\Lambda=0$, $\lambda=16.94$ ns^{-1}, and $\gamma=14$ ns. A typical channel impulse response from these parameters, as the one shown on Fig 2-bottom-left, has the same overall decay exponent and a similar net density of rays as in the previous case. The corresponding estimates of $\Lambda\Gamma$ and $\lambda\gamma$, obtained by applying the algorithm proposed in this section, are shown in the scatter plot of Fig 2-top-right. Here, for twelve sets of 4000 realizations of the channel impulse response, the corresponding twelve empirical estimates of $c(0,\omega)$ for for 500 values of ω evenly distributed

[4] If there were no clusters, the impulse response would be as if there were only a single cluster, beginning at $t=0$, with decay exponent Γ.

[5] In practice, it will also be necessary to identify the power scaling factor of the impulse response, namely, the value of $b_2(T)$ at $T=0$. This can be easily done by taking the empirical mean of the squared magnitude of the first ray in the impulse response.

[6] About 4000 channel realizations was found to be a sufficiently large data set size in order to achieve this reliability. Please see also the discussed below on estimation accuracy.

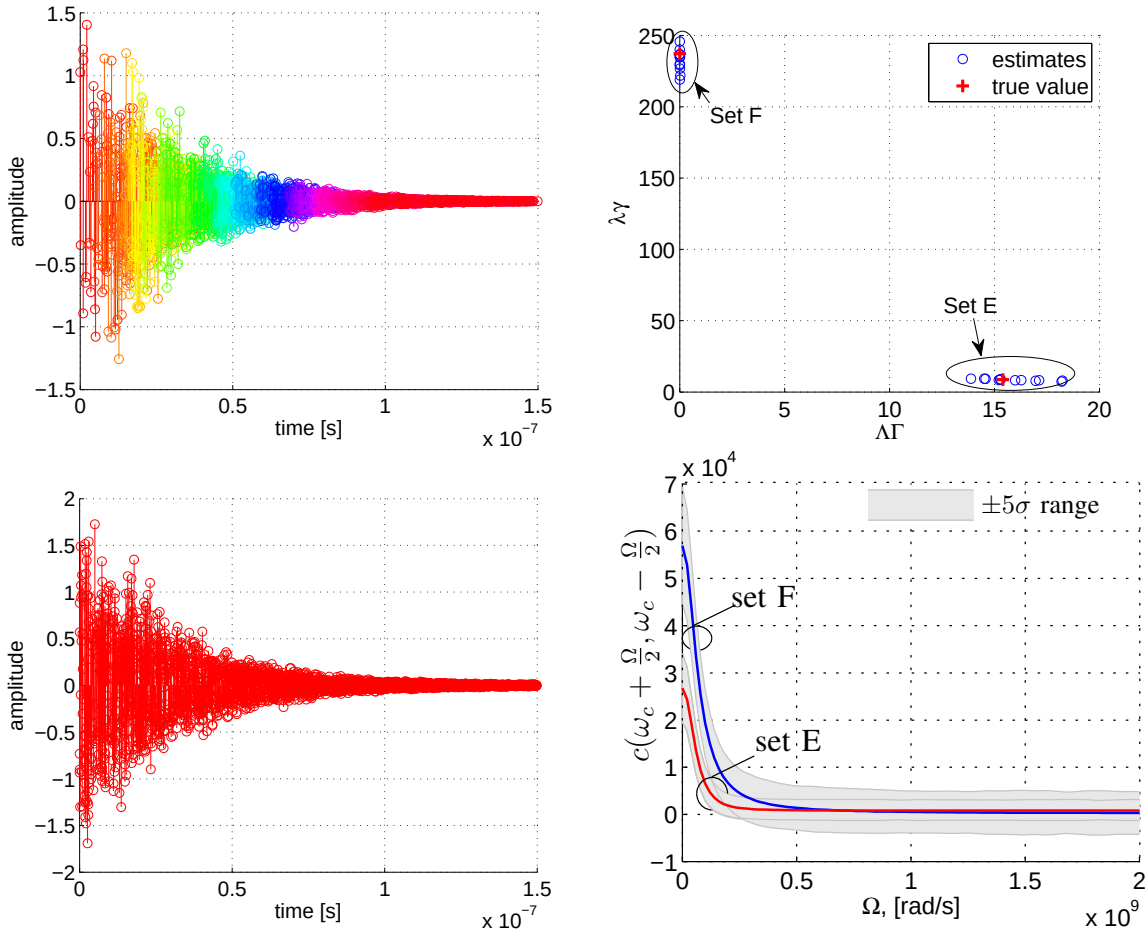

Figure 2: Left: Typical impulse response for the SV channel model with the parameters of set E ($\Lambda = 1.1$ ns^{-1}, $\lambda = 1.1$ ns^{-1}, $\Gamma = 14$ ns , $\gamma = 7.9$ ns), (top), and set F ($\Lambda = 0$, $\lambda = 16,94$ ns^{-1} , $\gamma = 14$ ns) (bottom). Multipath components from the same cluster are shown with the same color. Right-top: Twelve estimates of $\Lambda\Gamma$ and $\lambda\gamma$, each from 4000 realizations of the impulse responses for each set of parameters, obtained applying the method proposed in this section. Right-bottom: autocovariance of $|H(j\omega)|^2$ from (28) and $\pm 5\sigma$ ranges along them, where σ is the standard deviation of the empirical estimate of $c(\cdot,\cdot)$ from 4000 channel realizations.

over $[0\,,\,5\times10^9]$ rad/s, were obtained. Notice how, in all 100 realizations, the estimates of $\Lambda\Gamma$ are well below 3×10^{-2}, unambiguously revealing the absence of clusters.

The possibility of correctly estimating the true parameters of a channel (Λ, Γ, λ , γ in the SV case) from the empirical estimate of $c(\cdot,\cdot)$, say $\tilde{c}(\cdot,\cdot)$, averaged from N independent channel realizations, will ultimately depend upon the accuracy of the latter estimate. To illustrate this dependency, the theoretical autocovariance $c(\omega_c+\frac{\Omega}{2},\omega_c-\frac{\Omega}{2})$ is plotted in Fig. 2 right-bottom, for the parameter sets E and F. The regions within five standard deviations of the estimate $\tilde{c}$ above and below each of the $c(\omega_c+\frac{\Omega}{2},\omega_c-\frac{\Omega}{2})$ curves is shown as shaded areas. The standard deviation shown corresponds to what is obtained when $\tilde{c}(\cdot,\cdot)$ is calculated from $N = 4000$ channel realizations, the same number utilized to obtain the estimates shown in Fig. 2-top-right. Given the significant overlap of these regions, and since the variance of $\tilde{c}(\cdot,\cdot)$ is proportional to N^{-1}, it is clear that, in this case, a reliable decision about which of the parameter sets better fits the data cannot be achieved from much less than 4000 channel realizations.

We end this section by noting that the parameter estimation algorithm described above has been proposed for its simplicity and with the purpose of illustrating the potential applicability of the results derived in Sections III and IV. Therefore, the search for better estimation algorithms, which must certainly exist, goes beyond the scope of this paper.

E. Second-Order Statistics of Total Power Over a Band

The variance of the channel power over a band $\mathcal{B} \triangleq [\omega_l, \omega_r]$ rad/s is obtained by substituting (27) into (23), with the change of variables $v = \omega_l - u$ and $v = \omega_r + u$:

$$\begin{aligned} var(P_{\mathcal{B}}) &= W^2K + 2\int_0^W (W-v)\bar{c}(v)dv \\ &\quad + \int_{2\omega_l}^{2\omega_l+W} (v-2\omega_l)\bar{c}(v)dv \\ &\quad + \int_{2\omega_r-W}^{2\omega_r} (2\omega_r - v)\bar{c}(v)dv \\ &= W^2K \end{aligned}$$

$$+2\int_0^W (W-v)\left(\frac{K_1}{1/\gamma^2+v^2}+\frac{K_2}{1/\Gamma^2+v^2}\right)dv$$
$$+\int_{2\omega_l}^{2\omega_l+W}(v-2\omega_l)\left(\frac{K_1}{1/\gamma^2+v^2}+\frac{K_2}{1/\Gamma^2+v^2}\right)dv$$
$$+\int_{2\omega_r-W}^{2\omega_r}(2\omega_r-v)\left(\frac{K_1}{1/\gamma^2+v^2}+\frac{K_2}{1/\Gamma^2+v^2}\right)dv$$

Evaluating these integrals, using the change of variables $\omega_c \triangleq (\omega_l+\omega_r)/2$, and applying the identity $\arctan(x)+\arctan(y)=\arctan(\frac{x+y}{1-xy})$, we obtain, after some manipulation, that

$$\begin{aligned}var(P_{\mathcal{B}}) &= W^2K + 2WK_1\gamma\arctan(\gamma W)\\ &+ 2WK_2\Gamma\arctan(\Gamma W) - K_1\ln\left(1+\gamma^2W^2\right)\\ &- K_2\ln\left(1+\Gamma^2W^2\right)\\ &+ \tfrac{K_1}{2}\ln\left(\frac{[1+\gamma^2(2\omega_c)^2]^2}{(1+\gamma^2(2\omega_c-W)^2)(1+\gamma^2(2\omega_c+W)^2)}\right)\\ &+ \tfrac{K_2}{2}\ln\left(\frac{[1+\Gamma^2(2\omega_c)^2]^2}{(1+\Gamma^2(2\omega_c-W)^2)(1+\Gamma^2(2\omega_c+W)^2)}\right)\\ &+ K_1\gamma W\arctan\left(\frac{2\gamma W}{1+4\gamma^2\omega_c^2}\right)\\ &- 2K_1\gamma\omega_c\arctan\left(\frac{4\gamma^3\omega_c W^2}{[1+4\gamma^2\omega_c^2]^2+\gamma^2W^2[1-4\gamma^2\omega_c^2]}\right)\\ &+ K_2\Gamma W\arctan\left(\frac{2\Gamma W}{1+4\Gamma^2\omega_c^2}\right)\\ &- 2K_2\Gamma\omega_c\arctan\left(\frac{4\Gamma^3\omega_c W^2}{[1+4\Gamma^2\omega_c^2]^2+\Gamma^2W^2[1-4\Gamma^2\omega_c^2]}\right)\end{aligned} \tag{33}$$

The relative variability of $P_{\mathcal{B}}$ with respect to the average total power over $\mathcal{B}$ is better captured by the normalized variance

$$\frac{var(P_{\mathcal{B}})}{\mathrm{E}\left[P_{\mathcal{B}}\right]^2} = \frac{var(P_{\mathcal{B}})}{W^2(\Lambda\Gamma+1)^2(\lambda\gamma+1)^2}, \tag{34}$$

where the equality is obtained by substituting (24) and (14) into (12).

Equations (33) and (34) reveal several interesting aspects about the normalized channel power variance, which are discussed below:

i) Except for the first term on the RHS of (33), all the other terms grow sub-quadratically when W is above some frequency. It is a simple (although long) exercise of algebra to show that the frequency above which the growth rate with W of all these terms is significantly slower than W^2 is given by $W_{\text{sat}} \triangleq \gamma^{-1}\max\{1\ ,\ 0.5(1+(2\omega_c\gamma)^2)\}$. If $W \gg W_{\text{sat}}$, then the normalized variance of the total power over $\mathcal{B}$ can be well approximated as

$$\begin{aligned}\frac{var(P_{\mathcal{B}})}{\mathrm{E}\left[P_{\mathcal{B}}\right]^2} &\simeq \frac{K}{(\Lambda\Gamma+1)^2(\lambda\gamma+1)^2}\\ &= \frac{\frac{\Lambda\Gamma}{2}(\lambda\gamma+1)+(\frac{\Lambda\Gamma}{2}+1)}{(\Lambda\Gamma+1)^2(\lambda\gamma+1)}\end{aligned}$$

where we have used (26). Thus, in agreement with what was shown in Sections III-B1 and IV-B, the normalized variance of the power over an asymptotically infinite bandwidth vanishes only when the number of significant clusters tends to infinity.

ii) The narrow-band normalized channel power variance, $var(P_0)/\mathrm{E}\left[P_0\right]^2$ is obtained from (34) by letting $\Omega \to 0$. If W is small enough, then all the terms in (33) grow proportional to W^2. It is straightforward (but lengthy) to show that the maximum value for this to be a reasonable approximation is $W_{\text{flat}} \triangleq \Gamma^{-1}\min\{1,\ \sqrt{\Gamma\omega_c(1+\frac{\Gamma\omega_c}{1+\Gamma\omega_c})}\}$. When W is smaller than the latter threshold, it holds that

$$var(P_{\mathcal{B}}) \simeq \left(K + K_1\gamma^2 + K_2\Gamma^2 + K_1\frac{\gamma^2}{1+4\gamma^2\omega_c^2} + K_2\frac{\Gamma^2}{1+4\Gamma^2\omega_c^2}\right)W^2$$

and therefore

$$\frac{var(P_{\mathcal{B}})}{\mathrm{E}\left[P_{\mathcal{B}}\right]^2} \simeq \frac{K + K_1\gamma^2 + K_2\Gamma^2 + K_1\frac{\gamma^2}{1+4\gamma^2\omega_c^2} + K_2\frac{\Gamma^2}{1+4\Gamma^2\omega_c^2}}{(\Lambda\Gamma+1)^2(\lambda\gamma+1)^2} \tag{35}$$

Thus, unless the bandwidth W is comparable to or larger than W_{flat}, no reduction in normalized channel power gain variance is to be expected.

Notice also that if there is a single cluster with deterministic amplitude and infinite duration (i.e., if we let $\Gamma = 0$ and $\gamma \to \infty$), the narrow band normalized channel power variance should coincide with that of a Rayleigh channel (in which case $P_{\mathcal{B}}$ should distribute exponentially). Indeed, if we substitute the expressions for K_1 and K_2 in (35), fix $\Gamma = 0$ and let $\gamma \to \infty$, then it is easy to verify that $var(P_{\mathcal{B}})/\mathrm{E}\left[P_{\mathcal{B}}\right]^2 \to 1$, which is precisely the variance-to-squared-expectation ratio of an exponentially distributed random variable.

The curves in dashed line in Fig. 3 display the value of $var[P_{\mathcal{B}}]/\mathrm{E}\left[P_{\mathcal{B}}\right]^2$ for a band of width W centered at 10^9 [rad/s] obtained from 300,000 simulated realizations of the SV model for each set of parameters given in Table I. The corresponding values of $var[P_{\mathcal{B}}]/\mathrm{E}\left[P_{\mathcal{B}}\right]^2$ predicted by (34) are plotted in the same figure with solid lines. It can be seen that, in all cases, the theoretical and simulation curves are almost indistinguishable, confirming the accuracy of our results. It can also be seen that in all sets, as expected from (34), when W is increased from zero, the normalized channel power variance remains almost constant until a certain value, near the threshold W_{flat} defined previously. Beyond that threshold, all the curves decay with W until a saturation point is reached, in a way that is consistent with what was found in [13].

VI. Conclusions

We derived general expressions that characterize the second-order statistics of the frequency response power gain in

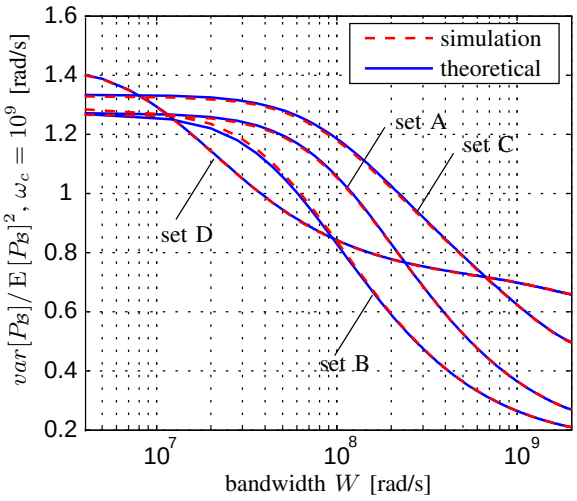

Figure 3: Normalized variance of the channel power gain over a band $\mathcal{B}$ of width W centered at 10^9 [rad/s], for the SV model with the four sets of parameters (A,B,C,D) given in Table I. Simulated values are averages over $3000,000$ channel realizations. The theoretical curve was obtained using (33) and (34).

wireless indoor channels. Our results are applicable to several well established channel models discussed in the literature, all based upon the Saleh-Valenzuela model [1]. In particular, the closed-form formula obtained here for the auto-covariance of the squared frequency response magnitude of the channel allows one to predict the variance of the aggregate channel power gain over any frequency band. This provides an approximation to the diversity order of wide-band over narrow-band systems in such channels. Our results also allow one to obtain an upper bound for this measure of spectral diversity, and show how (and why) this limit arises from having a finite number of clusters with significant amplitude in the channel impulse response. In addition, the derived formulas explicitly reveal how the statistical properties of the clusters in the channel impulse response affect the spectral autocovariance of the channel power gain. This allows one to use these spectral statistics to identify the presence or absence of clusters. A simple procedure to accomplish this task has been proposed and its effectiveness has been verified by applying it to simulated realizations of the Saleh-Valenzuela channel model.

VII. Appendix

A. Proof of Theorem 1

For notational simplicity, we will temporarily adopt a single indexing nomenclature for the path arrival times $\tau_{i,m}$. More precisely, and with a slight abuse of notation, we define the infinite random set $\{\tau_\ell\}_{\ell=1}^{\infty} \triangleq \{\{\tau_{i,m}\}_{m=1}^{\infty}\}_{i=1}^{\infty}$. For our purposes, it will not be necessary to define a mapping between the indexes i, m and the index ℓ. Indeed, it will be sufficient to note that the double-index matching condition $(i,m) = (j,n)$ (which means $i = j$ and $m = n$) is equivalent to the single-index condition $\ell = k$.

Using single-index notation, the first term on the right hand side of (13) is obtained from (9), which yields

$$\mathrm{E}[|H(\omega_1)|^2\,|H(\omega_2)|^2] = \sum_{\ell,k,l,r} \mathrm{E}\left[a_\ell a_k a_l a_r\, \mathrm{e}^{-j(\omega_1[\tau_\ell-\tau_k]+\omega_2[\tau_l-\tau_r])}\right] \quad (36)$$

Consider the cases in which r is different from all other coefficients. Then

$$\mathrm{E}\left[a_\ell a_k a_l a_r\, \mathrm{e}^{-j(\omega_1[\tau_\ell-\tau_k]+\omega_2[\tau_l-\tau_r])}\right] \overset{(a)}{=} \mathrm{E}\left[a_\ell a_k a_l A_r \alpha_r\, \mathrm{e}^{-j(\omega_1[\tau_\ell-\tau_k]+\omega_2[\tau_l-\tau_r])}\right]\mathrm{E}\,[p_r] \;=\; 0,$$

where (a) follows from (7) and the last equality stems from the fact that all $\{p_i\}$ have zero mean (see (3)). Proceeding similarly it is easy to show that each term in the summation of (36) in which one or more indexes is not matched to any other index evaluates to zero. Thus, one must only consider the cases $(\ell = k = l = r)$, $(\ell = k \neq l = r)$, $(\ell = l \neq k = r)$ and $(\ell = r \neq k = l)$, which yields, respectively, each of the following sums:

$$\begin{aligned}
&\mathrm{E}[|H(\omega_1)|^2\,|H(\omega_2)|^2] \\
&= \underbrace{\sum_{\ell} \mathrm{E}\left[a_\ell^4\right] + \sum_{\ell}\sum_{l:l\neq\ell} \mathrm{E}\left[a_\ell^2 a_l^2\right]}_{\mathcal{T}_1} \\
&\quad + \underbrace{\sum_{\ell}\sum_{k:k\neq\ell} \mathrm{E}\left[a_\ell^2 a_k^2\, \mathrm{e}^{-j([\omega_1+\omega_2][\tau_\ell-\tau_k])}\right]}_{\mathcal{T}_2(\omega_1+\omega_2)} \\
&\quad + \underbrace{\sum_{\ell}\sum_{k:k\neq\ell} \mathrm{E}\left[a_\ell^2 a_k^2\, \mathrm{e}^{-j([\omega_1-\omega_2][\tau_\ell-\tau_k])}\right]}_{\mathcal{T}_2(\omega_1-\omega_2)}
\end{aligned} \quad (37)$$

Rewriting the frequency-independent term $\mathcal{T}_1$ in double-index notation, we have

$$\begin{aligned}
\mathcal{T}_1 &= \sum_{i,m} \mathrm{E}\left[a_{i,m}^4\right] + \sum_{i,m}\sum_{(j,n)\neq(i,m)} \mathrm{E}\left[a_{i,m}^2 a_{j,n}^2\right] \\
&= \sum_{i,m} \mathrm{E}\left[a_{i,m}^4\right] + \sum_i \sum_m \sum_{n:n\neq m} \mathrm{E}\left[a_{i,m}^2 a_{i,n}^2\right] \\
&\qquad + \sum_i \sum_{j:j\neq i} \sum_m \sum_n \mathrm{E}\left[a_{i,m}^2 a_{j,n}^2\right] \\
&= \sum_{i,m} \mathrm{E}\left[A_i^4 \alpha_{i,m}^4\right] + \sum_i \sum_m \sum_{n:n\neq m} \mathrm{E}\left[A_i^4 \alpha_{i,m}^2 \alpha_{i,n}^2\right] \\
&\qquad + \sum_i \sum_{j:j\neq i} \sum_m \sum_n \mathrm{E}\left[A_i^2 A_j^2 \alpha_{i,m}^2 \alpha_{j,n}^2\right] \\
&\overset{(a)}{=} \sum_i \mathrm{E}\left[A_i^4\right] \left(\sum_m \mathrm{E}\left[\alpha_{i,m}^4\right] + \sum_m \sum_{n:n\neq m} \mathrm{E}\left[\alpha_{i,m}^2 \alpha_{i,n}^2\right] \right) \\
&\qquad + \sum_i \sum_{j:j\neq i} \mathrm{E}\left[A_i^2 A_j^2\right] \sum_m \mathrm{E}\left[\alpha_{i,m}^2\right] \sum_n \mathrm{E}\left[\alpha_{j,n}^2\right] \\
&\overset{(b)}{=} \int_0^\infty \bar{\lambda}_T(x) b_4(x) dx \left(\int_0^\infty \bar{\lambda}_t(t) g_4(x) dx \right.
\end{aligned}$$

$$+\int_0^\infty \int_{\substack{0\\ y\neq z}}^\infty \bar{\bar{\lambda}}_t(y,z) g_2(y) g_2(z) dy dz \Bigg)$$

$$+\int_0^\infty \int_{\substack{0\\ y\neq z}}^\infty \bar{\bar{\lambda}}_T(y,z) b_2(y) b_2(z) dy dz \left(\int_0^\infty \bar{\lambda}_t(x) g_2(x) dx\right)^2 \quad (38)$$

In the above, (a) is a consequence of the independence relationships established in (7), while (b) follows directly from Lemma 1. Proceeding similarly with the frequency-dependent function $T_2(\cdot)$, we obtain

$$\begin{aligned}
\mathcal{T}_2(\theta) &= \sum_\ell \sum_{k:k\neq\ell} \mathrm{E}\left[a_\ell^2 a_k^2 \,\mathrm{e}^{-j(\theta[\tau_\ell-\tau_k])}\right] \\
&= \sum_{i,m} \sum_{(j,n)\neq(i,m)} \mathrm{E}\left[a_{i,m}^2 a_{j,n}^2 \,\mathrm{e}^{-j(\theta[\tau_{i,m}-\tau_{j,n}])}\right] \\
&= \sum_{i,m} \sum_{(j,n)\neq(i,m)} \mathrm{E}\left[A_i^2 A_j^2 \alpha_{i,m}^2 \alpha_{j,n}^2 \,\mathrm{e}^{-j(\theta[T_i-T_j+t_{i,m}-t_{j,n}])}\right] \\
&= \sum_{i,m} \sum_{(j,n)\neq(i,m)} \mathrm{E}\left[A_i^2 A_j^2 \,\mathrm{e}^{-j(\theta[T_i-T_j])}\right] \times \\
&\qquad\qquad \mathrm{E}\left[\alpha_{i,m}^2 \alpha_{j,n}^2 \,\mathrm{e}^{-j\theta[t_{i,m}-t_{j,n}]}\right] \\
&= \sum_i \mathrm{E}\left[A_i^4\right] \sum_m \sum_{n:n\neq m} \mathrm{E}\left[\alpha_{i,m}^2 \alpha_{i,n}^2 \,\mathrm{e}^{-j\theta[t_{i,m}-t_{i,n}]}\right] \\
&+ \sum_i \sum_{j:j\neq i} \mathrm{E}\left[A_i^2 A_j^2 \,\mathrm{e}^{-j(\theta[T_i-T_j])}\right] \times \\
&\qquad \sum_m \sum_n \mathrm{E}\left[\alpha_{i,m}^2 \,\mathrm{e}^{-j\theta t_{i,m}}\right] \mathrm{E}\left[\alpha_{j,n}^2 \,\mathrm{e}^{j\theta t_{j,n}}\right] \\
&= \int_0^\infty \bar{\lambda}_T(x) b_4(x) dx \times \\
&\qquad \int_0^\infty \int_{\substack{0\\ y\neq z}}^\infty \bar{\bar{\lambda}}_t(y,z) g_2(y) g_2(z) \,\mathrm{e}^{-j(\theta[y-z])} \, dy dz \\
&+ \int_0^\infty \int_{\substack{0\\ y\neq z}}^\infty \bar{\lambda}_T(y) b_2(y) \bar{\lambda}_T(z) b_2(z) \,\mathrm{e}^{-j\theta[y-z]} \, dy dz \times \\
&\qquad\qquad \left|\int_0^\infty \bar{\lambda}_t(x) g_2(x) \,\mathrm{e}^{-j\theta x} \, dx\right|^2
\end{aligned}$$

Substitution of these expressions for $\mathcal{T}_1$ and $\mathcal{T}_2(\cdot)$ into (37) followed by inserting the result and (12) into (13) yields

$$\begin{aligned}
c(\omega_1,\omega_2) &= \int_0^\infty \bar{\lambda}_T(x) b_4(x) dx \times \\
&\quad \Bigg(\int_0^\infty \bar{\lambda}_t(t) g_4(x) dx + \int_0^\infty\int_0^\infty \bar{\bar{\lambda}}_t(y,z) g_2(y) g_2(z) dy dz \\
&\quad + \int_0^\infty\int_0^\infty \bar{\bar{\lambda}}_t(y,z) g_2(y) g_2(z) \,\mathrm{e}^{-j(\omega_1-\omega_2)(y-z)} \, dy dz \\
&\quad + \int_0^\infty\int_0^\infty \bar{\bar{\lambda}}_t(y,z) g_2(y) g_2(z) \,\mathrm{e}^{-j(\omega_1+\omega_2)(y-z)} \, dy dz \Bigg) \\
&\quad + \int_0^\infty\int_0^\infty \bar{\bar{\lambda}}_T(y,z) b_2(y) b_2(z) \,\mathrm{e}^{-j(\omega_1-\omega_2)[y-z]} \, dy dz \times \\
&\qquad\qquad \left|\int_0^\infty \bar{\lambda}_t(x) g_2(x) \,\mathrm{e}^{-j(\omega_1-\omega_2)x} \, dx\right|^2 \\
&\quad + \int_0^\infty\int_0^\infty \bar{\bar{\lambda}}_T(y,z) b_2(y) b_2(z) \,\mathrm{e}^{-j(\omega_1+\omega_2)[y-z]} \, dy dz \times \\
&\qquad\qquad \left|\int_0^\infty \bar{\lambda}_t(x) g_2(x) \,\mathrm{e}^{-j(\omega_1+\omega_2)x} \, dx\right|^2 \\
&\quad + \Bigg(\int_0^\infty\int_0^\infty \bar{\bar{\lambda}}_T(y,z) b_2(y) b_2(z) dy dz \\
&\quad - \left(\int_0^\infty \bar{\lambda}_T(T) b_2(T) dT\right)^2 \Bigg) \left(\int_0^\infty \bar{\lambda}_t(x) g_2(x) dx\right)^2
\end{aligned}$$

where Proposition 1 in the Appendix has been used. The last term in the latter expression is the difference between the rightmost term in (38) and the squared RHS of (12). Using the effective moment delay profile functions defined in (14), the auto-covariance of $|H(j\omega)|^2$ can be written as

$$\begin{aligned}
c(\omega_1,\omega_2) &= \|B_4\|_1 \left(\|G_4\|_1 + \|\Phi\|_1\right) \\
&\quad + \|B_4\|_1 \Big(\widehat{\Phi}([\omega_1-\omega_2], -[\omega_1-\omega_2]) \\
&\qquad + \widehat{\Phi}([\omega_1+\omega_2], -[\omega_1+\omega_2]) \Big) \\
&\quad + \widehat{\Psi}([\omega_1-\omega_2], -[\omega_1-\omega_2]) \left|\widehat{G}_2(\omega_1-\omega_2)\right|^2 \\
&\quad + \widehat{\Psi}([\omega_1+\omega_2], -[\omega_1+\omega_2]) \left|\widehat{G}_2(\omega_1+\omega_2)\right|^2 \\
&\quad + \left(\|\Psi\|_1 - \|B_2\|_1^2\right) \|G_2\|_1^2 \quad (39)
\end{aligned}$$

With the change of variables

$$\Omega \triangleq \omega_1 - \omega_2 \qquad\qquad \Theta \triangleq \omega_1 + \omega_2,$$

one can write (39) as (15), completing the proof. □

***Lemma** 1: Let $\{\mathrm{x}_k\}_{k=1}^\infty$ be an incrementally Markov random process, with x_1 possibly being deterministically equal to zero, and let $\{\varsigma_k\}_{k=1}^\infty$ be a random sequence i.i.d. under $\{\mathrm{x}_k\}_{k=1}^\infty$. Then, for any given $m \in \mathbb{N}$,*

$$\sum_{k=1}^\infty \mathrm{E}\left[\varsigma_k^m\right] = \int_0^\infty \bar{f}_m(x) \bar{\lambda}_{\mathrm{x}}(x) dx$$

$$\sum_{k=1}^\infty \sum_{\substack{j=1\\ j\neq k}}^\infty \mathrm{E}\left[\varsigma_k^m \varsigma_j^m\right] = \int_0^\infty \int_{\substack{0\\ y\neq z}}^\infty \bar{f}_m(y) \bar{f}_m(z) \bar{\bar{\lambda}}_{\mathrm{x}}(y,z) dy dz$$

provided the integrals exist, where

$$\bar{f}_m(x) \triangleq \begin{cases} \mathrm{E}\left[\varsigma_1^m\right], \text{ if } \mathrm{x}_1 = 0 \text{ deterministically and } x = 0, \\ \mathrm{E}\left[\varsigma_k^m | \, \mathrm{x}_k = x\right], k \in \{2, 3, \ldots\}, \text{if } \mathrm{x}_1 = 0 \\ \qquad\qquad\qquad\qquad \text{deterministically and } x \neq 0, \\ \mathrm{E}\left[\varsigma_k^m | \, \mathrm{x}_k = x\right], k \in \{1, 2, \ldots\}, \text{ if } \mathrm{x}_1 \text{ is random,} \end{cases}$$

is the m-th moment delay profile of $\{\varsigma_k\}_{k=1}^{\infty}$ and the single and joint effective arrival densities $\bar{\lambda}_{\mathrm{x}}(\cdot)$, $\bar{\bar{\lambda}}_{\mathrm{x}}(\cdot,\cdot)$ are as in Definition 3. ▲

Proof of Lemma 1: Let $f(x) \triangleq \mathrm{E}\left[\varsigma_k^m | \, \mathrm{x}_k = x\right]$, $k \in \mathbb{S}$, with $\mathbb{S}$ as in Definition 2. Recall the definitions of $\bar{\lambda}^{(i)}(x)$ and $\bar{\bar{\lambda}}^{(i)}(y,z)$ from (5). If $\mathrm{x}_1 = 0$ deterministically, then

$$\begin{aligned} \sum_{k=1}^{\infty} \mathrm{E}\left[\varsigma_k^m\right] &= \mathrm{E}[\varsigma_1^m] + \sum_{k=2}^{\infty} \mathrm{E}\left[f(\mathrm{x}_k)\right] \\ &\overset{(a)}{=} \mathrm{E}[\varsigma_1^m] + \int_0^{\infty} f(x) \bar{\lambda}_{\mathrm{x}}^{(2)}(x) dx \\ &= \int_0^{\infty} \bar{f}_m(x) \bar{\lambda}_{\mathrm{x}}(x) dx \end{aligned}$$

where (a) follows from Lemma 3 and (5), (4). Else,

$$\begin{aligned} \sum_{k=1}^{\infty} \mathrm{E}\left[\varsigma_k^m\right] = \sum_{k=1}^{\infty} \mathrm{E}\left[f(\mathrm{x}_k)\right] &= \int_0^{\infty} f(x) \bar{\lambda}_{\mathrm{x}}^{(1)}(x) dx \\ &= \int_0^{\infty} \bar{f}_m(x) \bar{\lambda}_{\mathrm{x}}(x) dx \end{aligned}$$

For the double sum in the lemma statement, if $\mathrm{x}_1 = 0$ deterministically, then

$$\begin{aligned} \sum_{k=1}^{\infty} \sum_{\substack{j=1 \\ j \neq k}}^{\infty} \mathrm{E}\left[\varsigma_k^m \varsigma_j^m\right] &= \mathrm{E}[\varsigma_1^m] \sum_{j=2}^{\infty} \mathrm{E}\left[f(\mathrm{x}_j)\right] \\ &\quad + \mathrm{E}[\varsigma_1^m] \sum_{k=2}^{\infty} \mathrm{E}\left[f(\mathrm{x}_k)\right] + \sum_{k=2}^{\infty} \sum_{\substack{j=2 \\ j \neq k}}^{\infty} \mathrm{E}\left[f(\mathrm{x}_k) f(\mathrm{x}_j)\right] \\ &\overset{(a)}{=} \mathrm{E}[\varsigma_1^m] \int_0^{\infty} f(y) \bar{\lambda}_{\mathrm{x}}^{(2)}(y) dy + \mathrm{E}[\varsigma_1^m] \int_0^{\infty} f(z) \bar{\lambda}_{\mathrm{x}}^{(2)}(z) dz \\ &\quad + \int_0^{\infty} \int_{\substack{0 \\ y \neq z}}^{\infty} f(y) f(z) \bar{\bar{\lambda}}_{\mathrm{x}}^{(2)}(y,z) dy dz \\ &\overset{(b)}{=} \int_0^{\infty} \int_{\substack{0 \\ y \neq z}}^{\infty} \bar{f}_m(y) \bar{f}_m(z) \Big[\bar{\bar{\lambda}}_{\mathrm{x}}^{(2)}(y,z) + \delta(y) \bar{\lambda}_{\mathrm{x}}^{(2)}(z) \\ &\quad + \delta(z) \bar{\lambda}_{\mathrm{x}}^{(2)}(y) \Big] dy dz, \end{aligned}$$

where (a) follows from Lemmas 3 and 4 (in the Appendix) and from (5), (4). In turn, (b) was obtained using the fact that $\bar{\lambda}^{(2)}(y)$ and $f(y)$ are bounded for $y = 0$.

Finally, if x_1 is random, it readily follows by applying Lemma 4 in the Appendix that

$$\begin{aligned} \sum_{k=1}^{\infty} \sum_{\substack{j=1 \\ j \neq k}}^{\infty} \mathrm{E}\left[\varsigma_k^m \varsigma_j^m\right] &= \sum_{k=1}^{\infty} \sum_{\substack{j=1 \\ j \neq k}}^{\infty} \mathrm{E}\left[f(\mathrm{x}_k) f(\mathrm{x}_j)\right] \\ &= \int_0^{\infty} \int_{\substack{0 \\ y \neq z}}^{\infty} f(y) f(z) \bar{\bar{\lambda}}_{\mathrm{x}}^{(1)}(y,z) dy dz \\ &= \int_0^{\infty} \int_{\substack{0 \\ y \neq z}}^{\infty} \bar{f}_m(y) \bar{f}_m(z) \bar{\bar{\lambda}}_{\mathrm{x}}(y,z) dy dz, \end{aligned}$$

which completes the proof. ■

Lemma 2: Let $c > 0$ be such that $\ln(1/c) > 2$. Then

$$\begin{aligned} \sum_{n=2}^{\infty} n c^n &\leq \frac{c}{\ln(1/c)} \left(\frac{1}{\ln(1/c)} + 1 \right) \\ \sum_{n=2}^{\infty} n^2 c^n &\leq \frac{c}{\ln(1/c)} \left[1 + \frac{2}{\ln(1/c)} \left(1 + \frac{1}{\ln(1/c)} \right) \right] \end{aligned}$$

Proof: We have that

$$\begin{aligned} \frac{d}{dx} x c^x &= (1 + x \ln c) c^x < 0 \iff x > 1/\ln(1/c) \\ \frac{d}{dx} x^2 c^x &= (2 + x \ln c) x c^x < 0 \iff x > 2/\ln(1/c) \end{aligned}$$

Then, since $\ln(1/c) > 2$,

$$\begin{aligned} \sum_{n=2}^{\infty} n c^n &\leq \int_1^{\infty} x c^x dx = -\frac{c}{\ln c} - \frac{1}{\ln c} \int_1^{\infty} \mathrm{e}^{x \ln c} dx \\ &= \frac{c}{\ln(1/c)} \left(1 + \frac{1}{\ln(1/c)} \right) \end{aligned}$$

Similarly,

$$\begin{aligned} \sum_{n=2}^{\infty} n^2 c^n &\leq \int_1^{\infty} x^2 c^x dx = -\frac{c}{\ln c} - \frac{2}{\ln c} \int_1^{\infty} x \, \mathrm{e}^{x \ln c} dx \\ &= \frac{c}{\ln(1/c)} \left[1 + \frac{2}{\ln(1/c)} \left(1 + \frac{1}{\ln(1/c)} \right) \right] \end{aligned}$$

■

Lemma 3: Let the arrival times $\{\mathrm{x}_i\}_{i=1}^{\infty}$ be an incrementally Markov sequence with x_1 randomly distributed. Define the function $\bar{\lambda} : \mathbb{R}_0^+ \mapsto \mathbb{R}_0^+$ as in (4). Then

$$\sum_{k=1}^{\infty} \mathrm{E}\left[g(\mathrm{x}_k)\right] = \int_0^{\infty} g(y) \bar{\lambda}(y) dy \tag{41}$$

▲

Proof: We have that

$$\begin{aligned}\sum_{k=1}^{\infty}\mathrm{E}\left[g(\mathrm{x}_k)\right] &= \mathrm{E}\left[\sum_{k=1}^{\infty} g(\mathrm{x}_k)\right]\\ &= \sum_{i=0}^{\infty}\mathrm{E}\left[\Delta^{-1}\sum\nolimits_{\mathrm{x}_k\in[i\Delta,i\Delta+\Delta)} g(\mathrm{x}_k)\right]\Delta\\ &= \lim_{\Delta\to 0}\sum_{i=0}^{\infty}\mathrm{E}\left[\Delta^{-1}\sum\nolimits_{\mathrm{x}_k\in[i\Delta,i\Delta+\Delta)} g(\mathrm{x}_k)\right]\Delta\\ &= \int_0^{\infty} g(x)\left(\lim_{\Delta\to 0}\frac{\mathrm{E}\left[\mathrm{n}_\Delta(x)\right]}{\Delta}\right)dx, \end{aligned} \tag{42}$$

where the discrete random variable $\mathrm{n}_\Delta(x)$ corresponds to the number of arrivals in $[x, x+\Delta)$. Its expectation satisfies

$$\begin{aligned}&\Pr\{\mathrm{n}_\Delta(x)=1\} \le \mathrm{E}\left[\mathrm{n}_\Delta(x)\right]\\ &\quad= \Pr\{\mathrm{n}_\Delta(x)=1\} + \sum_{n=2}^{\infty} n\Pr\{\mathrm{n}_\Delta(x)=n\}\\ &\quad\le \Pr\{\mathrm{n}_\Delta(x)=1\} + \Pr\{\mathrm{n}_\Delta(x)\ge 1\}\sum_{n=2}^{\infty} n[\rho\Delta]^{n-1}\\ &\quad\le \Pr\{\mathrm{n}_\Delta(x)=1\}\\ &\qquad+\Pr\{\mathrm{n}_\Delta(x)\ge 1\}\frac{1}{\ln\left(\frac{1}{\rho\Delta}\right)}\left[1+\frac{1}{\ln\left(\frac{1}{\rho\Delta}\right)}\right], \end{aligned} \tag{43}$$

where the last inequality follows from Lemma 2. Thus,

$$\begin{aligned}&\lim_{\Delta\to 0}\frac{\mathrm{E}\left[\mathrm{n}_\Delta(x)\right]}{\Delta} \le \lim_{\Delta\to 0}\frac{\Pr\{\mathrm{n}_\Delta(x)=1\}}{\Delta}\\ &+\lim_{\Delta\to 0}\left(\frac{\Pr\{\mathrm{n}_\Delta(x)\ge 1\}}{\Delta}\cdot\frac{1}{\ln\left(\frac{1}{\rho\Delta}\right)}\left[1+\frac{1}{\ln\left(\frac{1}{\rho\Delta}\right)}\right]\right)\\ &=\lim_{\Delta\to 0}\frac{\Pr\{\mathrm{n}_\Delta(x)=1\}}{\Delta}\end{aligned}$$

Hence

$$\lim_{\Delta\to 0}\frac{\mathrm{E}\left[\mathrm{n}_\Delta(x)\right]}{\Delta} = \lim_{\Delta\to 0}\frac{\Pr\{\mathrm{n}_\Delta(x)=1\}}{\Delta}$$

On the other hand,

$$\Pr\{\mathrm{n}_\Delta(x)=1\} \le \Pr\{\mathrm{n}_\Delta(x)\ge 1\} \le \mathrm{E}\left[\mathrm{n}_\Delta(x)\right]$$

Therefore,

$$\begin{aligned}\lim_{\Delta\to 0}\frac{P_\Delta^{(1)}(x)}{\Delta} &= \lim_{\Delta\to 0}\frac{\Pr\{\mathrm{n}_\Delta(x)=1\}}{\Delta}\\ &= \lim_{\Delta\to 0}\frac{\mathrm{E}\left[\mathrm{n}_\Delta(x)\right]}{\Delta}.\end{aligned} \tag{44}$$

Substitution of this result into (42) yields (41), completing the proof. ∎

Lemma 4: Let the arrival times $\{\mathrm{x}_k\}_{k=1}^{\infty}$ distribute as in Lemma 3, and define $\bar{\bar{\lambda}}(y,z)$ as in (4). Assume that $\bar{\bar{\lambda}}(y,z)$ is bounded for all $y, z \ge 0$, $y \ne z$. Then,

$$\sum_{k=1}^{\infty}\sum_{j\ne k}^{\infty}\mathrm{E}\left[g(\mathrm{x}_k)g(\mathrm{x}_j)\right] = \int_0^{\infty}\int_{\substack{0\\ y\ne z}}^{\infty} g(y)g(z)\bar{\bar{\lambda}}(y,z)dydz$$

Proof: We have that

$$\begin{aligned}&\sum_{k=1}^{\infty}\sum_{j\ne k}^{\infty}\mathrm{E}\left[g(\mathrm{x}_k)g(\mathrm{x}_j)\right] = \mathrm{E}\left[\sum_{k=1}^{\infty}\sum_{j\ne k}^{\infty} g(\mathrm{x}_k)g(\mathrm{x}_j)\right]\\ &= \sum_{i=0}^{\infty}\sum_{\ell=0}^{\infty}\mathrm{E}\left[\sum_{\mathrm{x}_k\in[i\Delta,i\Delta+\Delta)}\ \sum_{\substack{\mathrm{x}_j\in[\ell\Delta,\ell\Delta+\Delta)\\ j\ne k}} g(\mathrm{x}_k)g(\mathrm{x}_j)\right]\\ &= \sum_{i=0}^{\infty}\mathrm{E}\left[\sum_{\substack{\mathrm{x}_k,\mathrm{x}_j\in[i\Delta,i\Delta+\Delta)\\ j\ne k}} g(\mathrm{x}_k)g(\mathrm{x}_j)\right]\\ &+\sum_{i=0}^{\infty}\sum_{\ell:\ell\ne i}^{\infty}\mathrm{E}\left[\sum_{\mathrm{x}_k\in[i\Delta,i\Delta+\Delta)}\ \sum_{\mathrm{x}_j\in[\ell\Delta,\ell\Delta+\Delta)} g(\mathrm{x}_k)g(\mathrm{x}_j)\right]\\ &= \lim_{\Delta\to 0}\sum_{i=0}^{\infty}\mathrm{E}\left[\Delta^{-1}\sum_{\substack{\mathrm{x}_k,\mathrm{x}_j\in[i\Delta,i\Delta+\Delta)\Delta\\ j\ne k}} g(\mathrm{x}_k)g(\mathrm{x}_j)\right]\Delta\\ &+\lim_{\Delta\to 0}\sum_{i=0}^{\infty}\sum_{\ell:\ell\ne i}^{\infty}\mathrm{E}\left[\tfrac{1}{\Delta^2}\sum_{\mathrm{x}_k\in[i\Delta,i\Delta+\Delta)}\ \sum_{\mathrm{x}_j\in[\ell\Delta,\ell\Delta+\Delta)} g(\mathrm{x}_k)g(\mathrm{x}_j)\right]\Delta^2\\ &= \int_0^{\infty} g(x)^2\left(\lim_{\Delta\to\infty}\frac{\mathrm{E}[\mathrm{n}_\Delta(x)(\mathrm{n}_\Delta(x)-1)]}{\Delta}\right)dx\\ &\quad+\int_0^{\infty}\int_{\substack{0\\ y:y\ne z}}^{\infty} g(y)g(z)\left(\lim_{\Delta\to 0}\frac{\mathrm{E}\left[\mathrm{n}_\Delta(y)\,\mathrm{n}_\Delta(z)\right]}{\Delta^2}\right)dydz \end{aligned} \tag{45}$$

For the expectation within the first integral, we have

$$\begin{aligned}0 &\le \mathrm{E}[\mathrm{n}_\Delta(x)(\mathrm{n}_\Delta(x)-1)] = \mathrm{E}[(\mathrm{n}_\Delta(x))^2] - \mathrm{E}\left[\mathrm{n}_\Delta(x)\right]\\ &= \Pr\left\{\mathrm{n}_\Delta(x)=1\right\} + \sum_{n=2}^{\infty} n^2\Pr\left\{\mathrm{n}_\Delta(x)=n\right\} - \mathrm{E}\left[\mathrm{n}_\Delta(x)\right]\\ &\le \Pr\left\{\mathrm{n}_\Delta(x)=1\right\} + \sum_{n=2}^{\infty} n^2(\rho\Delta)^{n-1} - \mathrm{E}\left[\mathrm{n}_\Delta(x)\right]\end{aligned}$$

Dividing by Δ and taking the limit as $\Delta\to 0$, and then substituting (44) and applying Lemma 2, it follows that

$$\lim_{\Delta\to\infty}\frac{\mathrm{E}[\mathrm{n}_\Delta(x)(\mathrm{n}_\Delta(x)-1)]}{\Delta} = 0$$

On the other hand, for $z > y+\Delta$,

$$\begin{aligned}&\mathrm{E}\left[\mathrm{n}_\Delta(y)\,\mathrm{n}_\Delta(z)\right] = \Pr\{\mathrm{n}_\Delta(y)=1,\mathrm{n}_\Delta(z)=1\}\\ &\quad+\Pr\{\mathrm{n}_\Delta(y)=2,\mathrm{n}_\Delta(z)=1\}\\ &\quad+\sum_{n=1}^{\infty} n\Pr\{\mathrm{n}_\Delta(y)=n\}\sum_{m=2}^{\infty}\Pr\{\mathrm{n}_\Delta(z)=m|\,\mathrm{n}_\Delta(y)=n\}\\ &\le \Pr\{\mathrm{n}_\Delta(y)=1,\mathrm{n}_\Delta(z)=1\}\\ &\quad+\Pr\{\mathrm{n}_\Delta(z)=1|\,\mathrm{n}_\Delta(y)=2\}\Pr\{\mathrm{n}_\Delta(y)=2\}\\ &\quad+\Big(\Pr\{\mathrm{n}_\Delta(y)=1\}+\Pr\{\mathrm{n}_\Delta(y)\ge 1\}\sum_{n=2}^{\infty} n[\rho\Delta]^{n-1}\Big)\times\end{aligned}$$

$$\Pr\{\mathrm{n}_\Delta(z)\geq 1|\,\mathrm{n}_\Delta(y)\geq 1\}\sum_{m=2}^{\infty} m[\rho\Delta]^{m-1}$$
$$\leq \Pr\{\mathrm{n}_\Delta(y)=1,\mathrm{n}_\Delta(z)=1\}$$
$$+\Pr\{\mathrm{n}_\Delta(z)=1|\,\mathrm{n}_\Delta(y)\geq 1\}\Pr\{\mathrm{n}_\Delta(y)\geq 1\}\rho\Delta$$
$$+\Pr\{\mathrm{n}_\Delta(y)\geq 1,\mathrm{n}_\Delta(z)\geq 1\}\Big(1+\sum_{n=2}^{\infty} n[\rho\Delta]^{n-1}\Big)\times \sum_{m=2}^{\infty} m[\rho\Delta]^{m-1} \quad (46)$$

Noting that $\Pr\{\mathrm{n}_\Delta(y)=1,\mathrm{n}_\Delta(y)=1\}\leq \mathrm{E}\left[\mathrm{n}_\Delta(y)\,\mathrm{n}_\Delta(z)\right]$, that the integrand in (45) is symmetric in y and z, and proceeding with (46) as in (43), we conclude that

$$\lim_{\Delta\to 0}\frac{\mathrm{E}\left[\mathrm{n}_\Delta(y)\,\mathrm{n}_\Delta(z)\right]}{\Delta^2}=\lim_{\Delta\to 0}\frac{\Pr\{\mathrm{n}_\Delta(y)=1,\mathrm{n}_\Delta(y)=1\}}{\Delta^2} \quad (47)$$

Additionally, since

$$\Pr\{\mathrm{n}_\Delta(y)=1,\mathrm{n}_\Delta(z)=1\}\leq \Pr\{\mathrm{n}_\Delta(y)\geq 1,\mathrm{n}_\Delta(z)\geq 1\}$$
$$\leq \mathrm{E}\left[\mathrm{n}_\Delta(y)\,\mathrm{n}_\Delta(z)\right],$$

it follows from (47) that

$$\lim_{\Delta\to 0}\frac{\Pr\{\mathrm{n}_\Delta(y)=1,\mathrm{n}_\Delta(z)=1\}}{\Delta^2}$$
$$=\lim_{\Delta\to 0}\frac{\Pr\{\mathrm{n}_\Delta(y)\geq 1,\mathrm{n}_\Delta(z)\geq 1\}}{\Delta^2}$$
$$=\lim_{\Delta\to 0}\frac{\mathrm{E}\left[\mathrm{n}_\Delta(y)\,\mathrm{n}_\Delta(z)\right]}{\Delta^2}.$$

The proof is completed upon substituting this result into (45). ■

***Proposition** 1:* Let $\bar{\bar{\lambda}}_{\mathrm{x}}(y,z)$ be as in Definition 3 and let $f:\mathbb{R}\to\mathbb{R}$ be a bounded function. Then,

$$\int_0^\infty\int_{\substack{0\\ y\neq z}}^\infty \bar{\bar{\lambda}}_{\mathrm{x}}(y,z)f(y)f(z)dydz=\int_0^\infty\int_0^\infty \bar{\bar{\lambda}}_{\mathrm{x}}(y,z)f(y)f(z)dydz$$

▲

Proof: If x_1 is random, then $\bar{\bar{\lambda}}(y,z)$ is bounded, and the result follows trivially. Otherwise $\mathrm{x}_1=0$ deterministically, in which case

$$\int_0^\infty\int_{\substack{0\\ y\neq z}}^\infty \bar{\bar{\lambda}}_{\mathrm{x}}(y,z)f(y)f(z)dydz$$
$$=\int_0^\infty\int_{\substack{0\\ y\neq z}}^\infty f(y)f(z)\left[\bar{\bar{\lambda}}_{\mathrm{x}}^{(2)}(y,z)+\bar{\lambda}_{\mathrm{x}}^{(2)}(y)\delta(z)+\bar{\lambda}_{\mathrm{x}}^{(2)}(z)\delta(y)\right]dydz$$
$$=\int_0^\infty\int_0^\infty f(y)f(z)\bar{\bar{\lambda}}_{\mathrm{x}}^{(2)}(y,z)dydz$$
$$+\int_0^\infty f(z)\delta(z)\int_{\substack{0\\ y\neq z}}^\infty f(y)\bar{\lambda}_{\mathrm{x}}^{(2)}(y)dydz$$
$$+\int_0^\infty f(z)\bar{\lambda}_{\mathrm{x}}^{(2)}(z)\int_{\substack{0\\ y\neq z}}^\infty f(y)\delta(y)dydz$$
$$=\int_0^\infty\int_0^\infty f(y)f(z)\bar{\bar{\lambda}}_{\mathrm{x}}^{(2)}(y,z)dydz$$
$$+f(0)\int_{0^+}^\infty f(y)\bar{\lambda}_{\mathrm{x}}^{(2)}(y)dy+f(0)\int_{0^+}^\infty f(z)\bar{\lambda}_{\mathrm{x}}^{(2)}(z)dz$$
$$=\int_0^\infty\int_0^\infty f(y)f(z)\bar{\bar{\lambda}}_{\mathrm{x}}^{(2)}(y,z)dydz$$
$$+\int_0^\infty\int_0^\infty f(y)f(z)\bar{\lambda}_{\mathrm{x}}^{(2)}(y)\delta(z)dydz$$
$$+\int_0^\infty\int_0^\infty f(y)f(z)\bar{\lambda}_{\mathrm{x}}^{(2)}(z)\delta(y)dydz$$
$$=\int_0^\infty\int_0^\infty f(y)f(z)\bar{\bar{\lambda}}_{\mathrm{x}}(y,z)dydz,$$

completing the proof. ■

REFERENCES

[1] A. A. M. Saleh and R. A. Valenzuela, "A statistical model for indoor multipath propagation," *IEEE J. Sel. Areas Commun.*, vol. SAC-5, no. 2, pp. 128–137, Feb. 1987.

[2] J. Foerster *et al.*, "Channel Modeling Sub-comitee Report Final," IEEE, Tech. Rep., Feb. 2003, document IEEE 02490r0P802-15_SG3a.

[3] A. Molisch, F., K. Balakrishnan, D. Cassioli, C.-C. Chong, S. Emami, A. Fort, J. Karedal, J. Kunisch, H. Schantz, U. Schuster, and K. Siwiak, "IEEE 802.15.4.a channel model – final report," Feb. 2005. [Online]. Available: http://www.ieee802.org/15/pub/04/15-04-0662-02-004a-channel-model-final-report-r1.

[4] A. F. Molisch, "Ultrawideband propagation channels-theory, measurement, and modeling," *IEEE Trans. Veh. Technol.*, vol. 54, no. 5, pp. 1528–1545, Sept. 2005.

[5] A. Goldsmith, *Wireless communications*. New York: Cambridge University Press, 2005.

[6] X. Hong, C.-Z. Wang, J. Thompson, B. Allen, W. Q. Malik, and X. Ge, "On space-frequency correlation of UWB MIMO channels," *IEEE Trans. Veh. Technol.*, vol. 59, no. 9, pp. 4201–4213, Nov. 2010.

[7] M. Dohler, E. Okon, W. Malik, A. Brown, and D. Edwards, Eds., *Ultra-wideband: antennas and propagation for communications, radar and imaging*. John Wiley & Sons, 2007.

[8] F. Haber and M. R. Noorchashm, "Negatively correlated branches in frequency diversity systems to overcome multipath fading," vol. COMM-22, no. 2, pp. 180–190, Feb. 1974.

[9] S. Kozono, "Received signal-level characteristics in a wide-band mobile radio channel," *IEEE Trans. Veh. Technol.*, vol. 43, no. 3, pp. 480–486, Aug. 1994.

[10] F. D. Cardoso and L. M. Correia, "Fading depth dependence on system bandwidth in mobile communications – an analytical approach," *IEEE Trans. Veh. Technol.*, vol. 52, no. 3, pp. 587–594, May 2003.

[11] J. Yan and S. Kozono, "A study of received signal-level distribution in wideband transmission in mobile communications," *IEEE Trans. Veh. Technol.*, vol. 48, no. 5, pp. 1718–1725, Sept. 1999.

[12] G. Llano, J. Reig, and L. Rubio, "Analytical approach to model fade depth and fade margin in UWB channels," *IEEE Trans. Veh. Technol.*, vol. 59, no. 9, pp. 4214–4221, Nov. 2010.

[13] W. Q. Malik, B. Allen, and D. J. Edwards, "Bandwidth-dependent modelling of small-scale fade depth in wireless channels," *IET Microwaves, Antennas and Propagation*, vol. 2, no. 6, pp. 519–528, Sept. 2008.

[14] U. G. Schuster and H. Bölcskei, "Ultrawideband channel modeling on the basis of information-theoretic criteria," *IEEE Trans. Wireless Commun.*, vol. 6, no. 7, pp. 2464–2475, July 2007, available: http://www.nari.ee.ethz.ch/commth/pubs/p/schuster07-07a.

[15] A. M. Hayar, R. Knopp, and R. Saadane, "Subspace analysis of indoor UWB channels," *EURASIP J. Appl. Signal Process.*, vol. 3, pp. 287–295, 2005.

[16] A. F. Molisch *et al.*, "A comprehensive standardized model for ultrawideband propagation channels," *IEEE Trans. Antennas Propag.*, vol. 54, no. 11, pp. 3151–3166, Nov. 2006.

[17] H. Nakabayashi and S. Kozono, "Theoretical analysis of frequency-correlation coefficient for received signal level in mobile communications," *IEEE Trans. Veh. Technol.*, vol. 51, no. 4, pp. 729–737, July 2002.

[18] Q. Zhang and S. Song, "Exact expression for the coherence bandwidth of Rayleigh fading channels," *IEEE Trans. Commun.*, vol. 55, no. 7, pp. 1296–1299, July 2007.

[19] C.-C. Chong and S. Khiong Yong, "A generic statistical-based UWB channel model for high-rise apartments," *IEEE Trans. Antennas Propag.*, vol. 53, no. 8, pp. 2389–2397, Aug. 2005.

[20] M. S. Derpich and R. Feick, "On the second order power spectral statistics of wideband indoor microwave channels," in *Proc. PIMRC 2010*, Sept. 2010, pp. 335–340.

[21] M. Corrigan, A. Walton, N. Weihong, L. Jia, and T. Talty, "Automatic UWB clusters identification," in *Radio and Wireless Symp.*, Jan. 2009, pp. 376–379.

[22] B. Li, Z. Zhou, D. Li, and S. Zhai, "Efficient cluster identification for measured ultra-wideband channel impulse response in vehicle cabin," *Progress Electromagnetics Research*, vol. 117, pp. 121–147, 2011.

[23] A. F. Molisch, *Wireless Communications*. England: Wiley & Sons, 2005.

[24] K. Y. Yazdandoost and K. Syrafian-Pour, "Channel model for body area network (BAN)," document number EEEEP802.15-08-0780-09-0006, Apr. 2009. [Online]. Available: http://www.ieee802.org/15/pub/04/15-04-0662-02-004a-channel-model-final

[25] F. A. Haight, *Handbook of the Poisson distribution*. Wiley&Sons, 1967.

[26] W. Q. Malik, D. J. Edwards, and C. J. Stevens, "Frequency dependence of fading statistics for ultrawideband systems," *IEEE Trans. Wireless Commun.*, vol. 6, no. 3, pp. 800–804, Mar. 2007.

[27] G. Llano, J. Reig, and L. Rubio, "The UWB-OFDM channel analysis in frequency," in *Proc. IEEE Veh. Technol. Conf. (VTC 2009 Spring)*, 2009.

Milan S. Derpich (S'08–M'09) received the Ingeniero Civil Electrónico degree from the Universidad Técnica Federico Santa María (UTFSM), Valparaíso, Chile in 1999. During his time at the university he was supported by a full scholarship from the alumni association and upon graduating received several university-wide prizes. Mr. Derpich also worked by the electronic circuit design and manufacturing company Protonic Chile S.A. between 2000 and 2004. In 2009 he received the PhD degree in electrical engineering from the University of Newcastle, Australia. He received the Guan Zhao-Zhi Award at the Chinese Control Conference 2006, and the Research Higher Degrees Award from The Faculty of Engineering and Built Environment, University of Newcastle, Australia, for his PhD thesis. Since 2009 he has been with the Department of Electronic Engineering at Universidad Técnica Federico Santa María, Chile. His main research interests include rate-distortion theory, communications, networked control systems, sampling and quantization.

Rodolfo Feick (S'71-M'76-SM'95) obtained the degree of Ingeniero Civil Electrónico at Universidad Técnica Federico Santa María, Valparaíso, Chile in 1970 and the Ph.D. degree in Electrical Engineering at the University of Pittsburgh in 1975.

He has been with the Department of Electronics Engineering at Universidad Técnica Federico Santa María since 1975, where he is the head of the telecommunications area. His current interests include RF channel modeling, digital communications, microwave system design and RF measurement.